Turbulent biomagnetic fluid flow in a rectangular channel under the action of a localized magnetic field

E.E. Tzirtzilakis[†], M. Xenos[♣], V.C. Loukopoulos[*] and N.G. Kafoussias[†$]

[†]Department of Mathematics, Section of Applied Analysis, University of Patras, 26500 Patras, Greece.

[*]Department of Physics, University of Patras, 26500 Patras, Greece.

[♣]University of Illinois at Chicago, Department of Chemical Engineering 810 Clinton Str., Chicago, IL, 60607, U.S.A.

[+]e-mails: tzirtzi@iconography.gr, [♣]xenos@uic.edu, [*]vxloukop@physics.upatras.gr, [†]nikaf@math.upatras.gr

$ Corresponding author. Tel./fax: +30-2610997396.
E-mail address: nikaf@math.upatras.gr (N.G.Kafoussias)

Abstract

The fundamental problem of the turbulent flow of a biomagnetic fluid (blood) between two parallel plates under the action of a localized magnetic field is studied. The blood is considered to be an electrically conducting, incompressible and Newtonian fluid and its flow is steady, two-dimensional and turbulent. The turbulent flow is described by the Reynolds Averaged Navier-Stokes (RANS) equations. For the numerical solution of the problem under consideration, which is described by a coupled and non linear system of PDEs, with appropriate boundary conditions, the stream function-vorticity formulation is used. For the eddy-kinematic viscosity, the low Reynolds number k-ε turbulence model is adopted. The solution of the problem, for different values of the dimensionless parameter entering into it, is obtained by developing and applying an efficient numerical technique based on finite differences scheme. Results concerning the velocity and temperature field, skin friction and rate of heat transfer, indicate that the presence of the localized magnetic field, appreciable influences the turbulent flow field. A comparison is also made with the corresponding laminar flow, indicating that the influence of the magnetic field decreases in the presence of turbulence.

Keywords: Turbulent blood flow, magnetic field, FHD, MHD, BFD.

1. Introduction

In the last decades there is an increasing research activity concerning the use of the magnetic field in Biomechanics and Biomedicine applications. The use of the magnetic field seems to constitute an attractive prospect since it has been proposed for various non-invasive therapeutic techniques. Among the most popular applications, there are some concerning biocompatible magnetic nanoparticles, that may be used as a delivery system for anticancer agents in localized tumor therapy, called “magnetic drug targeting” [1]~[5]. Applications concerning the use of magnetic field are also proposed for cell separation [6], for therapy, such as hyperthermia or anticancer treatment [7], [8] and for the development of medical devices, such as blood pumps [9].

Among these studies there is a category concerning the study of the influence of the magnetic field on the flow of biological fluids. The biofluids, the flow of which is affected by the application of the magnetic field, are called biomagnetic fluids. One of the most interesting biomagnetic fluids is blood. The magnetic behavior of blood has been studied in several studies. This magnetic behavior appears due to the erythrocytes, which orient with their disk plane parallel to the magnetic field [10] ~ [14]. In fact, blood itself behaves like a diamagnetic material when oxygenated and paramagnetic when deoxygenated [15].

The effect of the magnetic field on pure blood is very weak and in order to affect its flow, strong magnetic fields are required. Thus, in several biomedical applications, such as magnetic drug targeting, artificially created magnetic nanoparticles are added to blood [16]. In that case, the effect of the magnetic field on blood flow increases dramatically as long as its magnetization increases several orders of magnitude. Consequently, blood with the addition of magnetic particles, except from paramagnetic or diamagnetic material, can be considered as a ferromagnetic fluid.

The first formulation of Biomagnetic Fluid Dynamics (BFD), for the investigation of the flow of a biofluid under the influence of an applied magnetic field (biomagnetic fluid flow), has been developed by Haik et. al [17]. According to this formulation the biomagnetic fluid is actually considered to possess the magnetic properties of blood. The blood in that BFD formulation is considered as a homogeneous, Newtonian, electrically **non**-conducting magnetic fluid. Clearly, the mathematical model of Haik et. al is valid for laminar blood flow in large vessels where the Newtonian behavior is a good approximation [18], [19]. Moreover, the BFD model is actually based on the one of FerroHydroDynamics (FHD) [20] ~ [26], which deals with no induced electric current and considers that the flow is affected by the magnetization of the fluid in the magnetic field [16], [17], [27].

However, blood also exhibits considerably high static electrical conductivity [28] ~ [30], due to the ions in the plasma. As the blood flows, electric current is generated and interacts with the magnetic field. Thus, the Lorentz force arises according to the principles of MagnetoHydroDynamics (MHD) [31] ~ [33]. This force depends on the magnetic field intensity itself (not gradient) and is considerable in areas where strong magnetic field is applied. Thus, an extended mathematical model of BFD, taking into account the electrical conductivity of blood, has been proposed in [34]. This model is derived by adopting the principles of both MHD and FHD and takes into account both magnetization and electrical conductivity of blood.

The physical problem of the laminar biofluid (blood) flow in a channel, under the action of a strong localized magnetic field, using similar considerations as in [34], has been studied in [35]. The same physical problem, using a different kind of magnetic field and adopting the model of BFD proposed by Haik et. al [17], has also been studied in [36].

Moderate and severe flow stenosis can produce highly disturbed flow regions with transitional and/or turbulent flow characteristics. Numerical investigations and experimental measurements showed that as the degree of stenosis is increased, and thus the disturbances in the flow domain become more intense, the critical Reynolds number is decreased. The flow, depending on the degree of stenosis, can become turbulent even for very low Reynolds numbers such that 230 or 300 [37] ~ [41]. The obtained results in various BFD flow problems showed that in all cases, the magnetic field causes the generation of strong vortices in the flow domain and effects similar to those generating in flow in stenotic vessels. Moreover, for some values of the parameters, the flow field is much more disturbed than that caused by a stenotic region [34] ~ [36]. Consequently, under such circumstances, the flow should be considered as turbulent even for low values of the Reynolds number.

Hence, in this work, the fundamental problem of a biomagnetic fluid (blood) turbulent flow between two parallel plates under the action of a localized magnetic field is studied. Blood is considered to be an incompressible, Newtonian and electrically conducting fluid and its flow turbulent, two-dimensional and steady. A similar physical problem, for laminar flow, has already been investigated in [35]. The mathematical model used in the present work is the extended BFD model presented in [34] and the turbulent model used is the k-ε turbulent model for low Re numbers. For the numerical solution of the PDEs, describing the problem under consideration, the stream function-vorticity formulation is adopted. The solution of the problem is obtained, numerically, by developing and applying an iterative scheme, which constitutes a combination of the numerical techniques used and described in detail in [34], [35] and [36].

Results concerning the fundamental physical quantities of the turbulent flow field, indicate that the presence of the localized magnetic field, appreciable influences them. It is worth mentioning, that for special values of some parameters, the system of equations that governs the turbulent flow in the channel, becomes the one that governs the laminar flow studied in [35]. Consequently, for the purpose of comparison, results are also obtained for the case of laminar flow, similar to those obtained in [35]. The results concerning the velocity, indicate that the presence of magnetic field appreciably influence the flow field in the laminar as well as in the turbulent flow. The major effect on the flow is the formation of two vortices in the area of the application of the magnetic field. The temperature is also increasing within the area where the magnetic field is applied. The influence of the magnetic field significantly reduces in the presence of turbulence.

2. Mathematical Formulation

The viscous, steady, two-dimensional, incompressible, turbulent biomagnetic fluid (blood) flow is considered taking place between two parallel flat plates (channel). The length of the plates is $\bar{L}$ and the distance between them is $\bar{h}$. The flow at the entrance is assumed to be fully developed and the upper plate is kept at constant temperature $\bar{T}_u$, whereas, the lower at temperature $\bar{T}_l$, such that $\bar{T}_l < \bar{T}_u$. The origin of the Cartesian coordinate system is located at the leading edge of the lower plate (see Figure 1).

For the fluid (blood) flow the following assumptions are made. The blood is considered to be an electrically conducting biomagnetic Newtonian fluid. The flow is considered to be turbulent and the increment of the viscosity due to the magnetic field is considered to be negligible. Also, the rotational forces acting on the erythrocytes, when entering and exiting the magnetic field are discarded (equilibrium magnetization). The assumption of equilibrium magnetization, even though is a considerable simplification, is a valid assumption for blood [27]. The walls of the channel are assumed electrically non-conducting and no electric field is applied.

The flow is subject to a locally applied magnetic field, which acts in the region of the interval defined by the points $(\bar{x}_1, 0)$ and $(\bar{x}_2, 0)$. The magnetic field strength intensity $\bar{H}$ is considered to be independent of y and is given by the expression [35]

$$\bar{H}(\bar{x}) = \frac{\bar{H}_0}{2}\,(\tanh[a_1(\bar{x}-\bar{x}_1)] - \tanh[a_2(\bar{x}-\bar{x}_2)])\,, \qquad (1)$$

where $\bar{H}_0$ is the magnetic field strength at the point $\bar{x}_0 = (\bar{x}_1 + \bar{x}_2)/2$, ($\bar{B}_0 = \bar{\mu}_0 \bar{H}_0$) and the coefficients a_1 and a_2 determine the magnetic field gradient at the points $\bar{x}_1$ and $\bar{x}_2$, respectively (see Figure 1).

For the magnetization $\bar{M}$, the following equation is used, involving the magnetic intensity $\bar{H}$ and the fluid temperature $\bar{T}$. That is

$$\bar{M} = \bar{K}\bar{H}\left(\bar{T}_c - \bar{T}\right). \qquad (2)$$

where $\bar{K}$ and $\bar{T}_c$ are constants [34]~[36] and [42].

Following these considerations, as the biofluid enters (area of $\bar{x}_1$ point) and leaves (area of $\bar{x}_2$ point) the region where the locally applied magnetic field acts and where the gradient of the magnetic field strength is high, the force due to magnetization, as well as the Lorentz force, arise. In the aforementioned area the magnetization force is expected to prevail and the Lorentz force is negligible. In the region where the magnetic field is almost uniform (area of $\bar{x}_0$ point), the Lorentz force prevails and the magnetization force becomes zero. Due to the way the magnetic field is applied, the gradient of the magnetic field strength exists only along the $\bar{x}$ direction, whereas it is zero along the $\bar{y}$ direction.

For the turbulent flow formulation, it is necessary to replace in the Navier Stokes equations, the instantaneous quantities by the sum of their mean value and fluctuating parts, e.g. for a dimensional quantity $\overline{f}$ it is written $\overline{f} = \tilde{\overline{f}} + \overline{f}'$. Hereafter, the mean values of the derived equations are considered. Finally, for the turbulent flow in the channel, the governing equations are the Reynolds Averaged Navier-Stokes equations (RANS), plus the additional terms of MHD and FHD [34], [35], expressing the influence of the applied magnetic field. Under these circumstances the equations governing the flow under consideration are:

$$\frac{\partial \tilde{\overline{u}}}{\partial \overline{x}} + \frac{\partial \tilde{\overline{v}}}{\partial \overline{y}} = 0\,, \tag{3}$$

$$\overline{\rho}\left(\tilde{\overline{u}}\frac{\partial \tilde{\overline{u}}}{\partial \overline{x}} + \tilde{\overline{v}}\frac{\partial \tilde{\overline{u}}}{\partial \overline{y}}\right) = -\frac{\partial \tilde{\overline{p}}}{\partial \overline{x}} + \overline{\mu}_0 \overline{M}\frac{\partial \overline{H}}{\partial \overline{x}} - \overline{\sigma}\overline{B}^2\tilde{\overline{u}} + \overline{\mu}\left(\frac{\partial^2 \tilde{\overline{u}}}{\partial \overline{x}^2} + \frac{\partial^2 \tilde{\overline{u}}}{\partial \overline{y}^2}\right) - \overline{\rho}\frac{\partial\left(\widetilde{\overline{u}'\overline{v}'}\right)}{\partial \overline{y}}\,, \tag{4}$$

$$\overline{\rho}\left(\tilde{\overline{u}}\frac{\partial \tilde{\overline{v}}}{\partial \overline{x}} + \tilde{\overline{v}}\frac{\partial \tilde{\overline{v}}}{\partial \overline{y}}\right) = -\frac{\partial \tilde{\overline{p}}}{\partial \overline{y}} + \overline{\mu}\left(\frac{\partial^2 \tilde{\overline{v}}}{\partial \overline{x}^2} + \frac{\partial^2 \tilde{\overline{v}}}{\partial \overline{y}^2}\right) - \overline{\rho}\frac{\partial\left(\widetilde{\overline{u}'\overline{v}'}\right)}{\partial \overline{x}}\,, \tag{5}$$

$$\begin{aligned}\overline{\rho}\;\overline{c}_p\left(\tilde{\overline{u}}\frac{\partial \tilde{\overline{T}}}{\partial \overline{x}} + \frac{\partial\left(\widetilde{\overline{T}'\overline{u}'}\right)}{\partial \overline{x}} + \tilde{\overline{v}}\frac{\partial \tilde{\overline{T}}}{\partial \overline{y}} + \frac{\partial\left(\widetilde{\overline{T}'\overline{v}'}\right)}{\partial \overline{y}}\right) - \overline{\mu}_0\overline{K}\overline{H}\tilde{\overline{T}}\left(\overline{u}\frac{\partial \overline{H}}{\partial \overline{x}} + \overline{v}\frac{\partial \overline{H}}{\partial \overline{y}}\right) \\ = \overline{k}\left(\frac{\partial^2 \tilde{\overline{T}}}{\partial \overline{x}^2} + \frac{\partial^2 \tilde{\overline{T}}}{\partial \overline{y}^2}\right) + \overline{\mu}_0\overline{K}\overline{H}\left(\left(\widetilde{\overline{u}'\overline{T}'}\right)\frac{\partial \overline{H}}{\partial \overline{x}} + \left(\widetilde{\overline{v}'\overline{T}'}\right)\frac{\partial \overline{H}}{\partial \overline{y}}\right) + \overline{\sigma}\overline{B}\tilde{\overline{u}}^2.\end{aligned} \tag{6}$$

The boundary conditions are:

Inflow conditions	$(\overline{x} = 0\,, 0 \le \overline{y} \le \overline{h})$:	$\tilde{\overline{u}} = \tilde{\overline{u}}(\overline{y})\,,\ \tilde{\overline{v}} = 0\,,\ \tilde{\overline{T}} = \tilde{\overline{T}}(\overline{y})$
Outflow conditions	$(\overline{x} = \overline{L}\,, 0 \le \overline{y} \le \overline{h})$:	$\partial(\tilde{\overline{R}})/\partial\overline{x} = 0$
Upper plate	$(\overline{y} = \overline{h}\,, 0 \le \overline{x} \le \overline{L})$:	$\tilde{\overline{u}} = 0\,,\ \tilde{\overline{v}} = 0\,,\ \tilde{\overline{T}} = \tilde{\overline{T}}_u$
Lower plate	$(\overline{y} = 0\,, 0 \le \overline{x} \le \overline{L})$:	$\tilde{\overline{u}} = 0\,,\ \tilde{\overline{v}} = 0\,,\ \tilde{\overline{T}} = \tilde{\overline{T}}_l$

For the derivation of the above equations, terms containing the mean value of a fluctuating quantity, e.g. $\tilde{\bar{f}}'$, as well as the terms of the form $\tilde{\bar{f}}'^2$ have been considered equal to zero.

In the above equations $\tilde{\bar{u}}$ and $\tilde{\bar{v}}$ are the mean values of the dimensional velocity components of the fluid in $\bar{x}$ and $\bar{y}$ direction, respectively, $\tilde{\bar{T}}$ is the mean value of temperature and $\tilde{\bar{p}}$ of pressure. $\bar{\rho}$ is the biomagnetic fluid density, $\bar{\mu}$ is the dynamic viscosity, $\bar{\mu}_o$ is the magnetic permeability of vacuum, σ is the electrical conductivity of biofluid, $\bar{c}_p$ is the specific heat at constant pressure, $\bar{k}$ is the thermal conductivity, $\bar{H}$ is the magnetic field strength, $\bar{B}$ is the magnetic induction ($\bar{B} = \bar{\mu}_o \bar{H}$). It is reminded that the bar above the quantities denotes that they are dimensional. On the other hand $\bar{u}(\bar{y})$ is a parabolic velocity profile corresponding to fully developed flow, $\bar{T}(\bar{y})$ is a linear profile and $\bar{R}$ stands for $\bar{T}$, $\bar{u}$ or $\bar{v}$.

The term $\bar{\mu}_o \bar{M}\, \partial\bar{H}/\partial\bar{x}$ in (4), represents the component of the magnetic force, per unit volume, and depend on the existence of the magnetic gradient.

The terms $\bar{\mu}_0 \bar{K}\bar{H}\tilde{\bar{T}}\left(\bar{u}\dfrac{\partial\bar{H}}{\partial\bar{x}} + \bar{v}\dfrac{\partial\bar{H}}{\partial\bar{y}}\right)$, $\bar{\mu}_0 \bar{K}\bar{H}\left(\left(\widetilde{\bar{u}'\bar{T}'}\right)\dfrac{\partial\bar{H}}{\partial\bar{x}} + \left(\widetilde{\bar{v}'\bar{T}'}\right)\dfrac{\partial\bar{H}}{\partial\bar{y}}\right)$ in equation (6), represent the thermal power per unit volume, due to the magnetocaloric effect. These two terms are widely used in FHD [20] ~ [26].

The term $\bar{\sigma}\bar{B}^2\tilde{\bar{u}}$ appearing in (4), represents the Lorentz force, per unit volume, and is arising due to the electrical conductivity of the fluid, whereas the term $\bar{\sigma}\bar{B}\tilde{\bar{u}}^2$ in (6) represents the Joule heating. These two terms arise in MHD [31] ~ [33].

For the dimensionless eddy kinematic viscosity ε_m and for the turbulent Prandtl number Pr_τ the following expressions are used:

$$\varepsilon_m = \bar{v}_\tau / \bar{v}\,, \qquad -\widetilde{\bar{u}'\bar{v}'} = \bar{v}_\tau\left(\frac{\partial\tilde{\bar{u}}}{\partial\bar{y}} + \frac{\partial\tilde{\bar{v}}}{\partial\bar{x}}\right) \tag{7}$$

and

$$-\widetilde{\bar{T}'\bar{v}'} = \frac{\bar{v}_\tau}{Pr_\tau}\frac{\partial\tilde{\bar{T}}}{\partial\bar{y}} \qquad -\widetilde{\bar{T}'\bar{u}'} = \frac{\bar{v}_\tau}{Pr_\tau}\frac{\partial\tilde{\bar{T}}}{\partial\bar{x}} \tag{8}$$

where, $\bar{v}_\tau$ is the turbulent kinematic viscosity and $\bar{v}$ is the kinematic viscosity [43].

Substituting the above quantities into equations (3)~(6), using the continuity equation and discarding the notation for the mean value above the quantities, the equations finally become:

$$\frac{\partial\bar{u}}{\partial\bar{x}}+\frac{\partial\bar{v}}{\partial\bar{y}}=0 \tag{9}$$

$$\frac{1}{\bar{\nu}}\left(\bar{u}\frac{\partial\bar{u}}{\partial\bar{x}}+\bar{v}\frac{\partial\bar{u}}{\partial\bar{y}}\right)=-\frac{1}{\bar{\rho}\bar{\nu}}\frac{\partial\bar{p}}{\partial\bar{x}}+\frac{\bar{\mu}_0}{\bar{\mu}}\bar{M}\frac{\partial\bar{H}}{\partial\bar{x}}-\frac{\bar{\sigma}}{\bar{\mu}}\bar{B}^2\bar{u}+\frac{\partial}{\partial\bar{y}}\left(\left(\varepsilon_m-1\right)\frac{\partial\bar{v}}{\partial\bar{x}}+\left(\varepsilon_m+1\right)\frac{\partial\bar{u}}{\partial\bar{y}}\right), \tag{10}$$

$$\frac{1}{\bar{\nu}}\left(\bar{u}\frac{\partial\bar{v}}{\partial\bar{x}}+\bar{v}\frac{\partial\bar{v}}{\partial\bar{y}}\right)=-\frac{1}{\bar{\rho}\bar{\nu}}\frac{\partial\bar{p}}{\partial\bar{y}}+\frac{\partial}{\partial\bar{x}}\left(\left(\varepsilon_m+1\right)\frac{\partial\bar{v}}{\partial\bar{x}}+\left(\varepsilon_m-1\right)\frac{\partial\bar{u}}{\partial\bar{y}}\right), \tag{11}$$

$$\begin{aligned}&\frac{\bar{\rho}^2\bar{c}_p}{\bar{\mu}}\left(\bar{u}\frac{\partial\bar{T}}{\partial\bar{x}}+\bar{v}\frac{\partial\bar{T}}{\partial\bar{y}}\right)-\frac{\bar{\rho}\bar{\mu}_0\bar{K}\bar{H}}{\bar{\mu}}\bar{T}\left(\bar{u}\frac{\partial\bar{H}}{\partial\bar{x}}+\bar{v}\frac{\partial\bar{H}}{\partial\bar{y}}\right)\\&=\bar{\rho}\bar{c}_p\frac{\partial}{\partial\bar{x}}\left[\left(\frac{1}{\Pr}+\frac{\varepsilon_m}{\Pr_\tau}\right)\frac{\partial\bar{T}}{\partial\bar{x}}\right]+\bar{\rho}\bar{c}_p\frac{\partial}{\partial\bar{y}}\left[\left(\frac{1}{\Pr}+\frac{\varepsilon_m}{\Pr_\tau}\right)\frac{\partial\bar{T}}{\partial\bar{y}}\right]-\bar{\mu}_0\bar{K}\bar{H}\frac{\varepsilon_m}{\Pr_\tau}\left(\frac{\partial\bar{T}}{\partial\bar{x}}\frac{\partial\bar{H}}{\partial\bar{x}}+\frac{\partial\bar{T}}{\partial\bar{y}}\frac{\partial\bar{H}}{\partial\bar{y}}\right)+\bar{\sigma}\bar{B}\bar{u}^2.\end{aligned} \tag{12}$$

The boundary conditions are:

$$\left.\begin{array}{lll}\text{Inflow conditions} & (\bar{x}=0,\,0\le\bar{y}\le\bar{h}): & \bar{u}=\bar{u}(\bar{y}),\ \bar{v}=0,\ \bar{T}=\bar{T}(\bar{y})\\ \text{Outflow conditions} & (\bar{x}=\bar{L},\,0\le\bar{y}\le\bar{h}): & \partial(\bar{R})/\partial\bar{x}=0,\end{array}\right\}$$

$$\begin{array}{lll}\text{Upper plate} & (\bar{y}=\bar{h},\,0\le\bar{x}\le\bar{L}): & \bar{u}=0,\ \bar{v}=0,\ \bar{T}=\bar{T}_u\\ \text{Lower plate} & (\bar{y}=0,\,0\le\bar{x}\le\bar{L}): & \bar{u}=0,\ \bar{v}=0,\ \bar{T}=\bar{T}_l\end{array} \tag{13}$$

3. Transformation of equations

In the system of (9)~(12) with boundary conditions (13) and the assumptions (1) and (2), the following non dimensional variables are introduced

$$x=\frac{\bar{x}}{\bar{h}},\quad y=\frac{\bar{y}}{\bar{h}},\quad u=\frac{\bar{u}}{\bar{u}_r},\quad v=\frac{\bar{v}}{\bar{u}_r}\quad p=\frac{\bar{p}}{\bar{\rho}\bar{u}_r^2},\quad H=\frac{\bar{H}}{\bar{H}_o},\quad T=\frac{\bar{T}-\bar{T}_l}{\bar{T}_u-\bar{T}_l}, \tag{14}$$

where $\bar{u}_r$ is the maximum velocity at the entrance.

For the numerical solution the stream function-vorticity formulation is adopted by introducing the dimensionless vorticity function J=J(x,y) and the dimensionless stream function Ψ=Ψ(x,y) defined by the expressions

$$J(x,y) = \frac{\partial v}{\partial x} - \frac{\partial u}{\partial y}, \tag{15}$$

$$u = \frac{\partial \Psi}{\partial y}, \qquad v = -\frac{\partial \Psi}{\partial x}. \tag{16}$$

Thus, equation (9) is automatically satisfied and equations (10), (11) and (12) produce, by eliminating the pressure p from the first two and substituting (16) in (12) and (15), the following system of equations

$$\nabla^2 \Psi = -J \tag{17}$$

$$\begin{aligned} &\nabla^2 J + \frac{2}{B}\left\{\frac{\partial J}{\partial x}\frac{\partial \varepsilon_m}{\partial x} + \frac{\partial J}{\partial y}\frac{\partial \varepsilon_m}{\partial y}\right\} - \frac{Re}{B}\left\{\frac{\partial J}{\partial x}\frac{\partial \Psi}{\partial y} - \frac{\partial J}{\partial y}\frac{\partial \Psi}{\partial x}\right\} = \\ &-\frac{1}{B}\left[2(A+B)\frac{\partial^4 \Psi}{\partial x^2 \partial y^2} + 4\left(\frac{\partial \varepsilon_m}{\partial y}\frac{\partial^3 \Psi}{\partial x^2 \partial y} + \frac{\partial \varepsilon_m}{\partial x}\frac{\partial^3 \Psi}{\partial x \partial y^2}\right) + \left(\frac{\partial^2 \varepsilon_m}{\partial x^2} - \frac{\partial^2 \varepsilon_m}{\partial y^2}\right)\left(\frac{\partial^2 \Psi}{\partial y^2} - \frac{\partial^2 \Psi}{\partial x^2}\right)\right. \\ &\qquad \left. + Mn_F Re\, H \frac{\partial H}{\partial x}\frac{\partial T}{\partial y} + Mn_M H^2 \frac{\partial^2 \Psi}{\partial y^2}\right] \end{aligned} \tag{18}$$

$$\begin{aligned} &\nabla^2 T + \frac{1}{A_0}\left\{\frac{\partial A_0}{\partial x}\frac{\partial T}{\partial x} + \frac{\partial A_0}{\partial y}\frac{\partial T}{\partial y}\right\} - \frac{Re}{A_0}\left\{\frac{\partial T}{\partial x}\frac{\partial \Psi}{\partial y} - \frac{\partial T}{\partial y}\frac{\partial \Psi}{\partial x}\right\} = \\ &= -Mn_F Re\, Ec\, H\, (\theta + T)\left\{\frac{\partial H}{\partial x}\frac{\partial \Psi}{\partial y}\right\} + \frac{\varepsilon_m}{Pr_\tau A_0} Mn_F Ec H \frac{\partial H}{\partial x}\frac{\partial T}{\partial x} - \frac{Mn_M Ec}{A_0} H^2 \left(\frac{\partial \Psi}{\partial y}\right)^2 \end{aligned} \tag{19}$$

where ∇^2 is the two dimensional Laplacian operator ($\nabla^2 = \vec{\nabla}\cdot\vec{\nabla} = \left(\partial^2/\partial x^2 + \partial^2/\partial y^2\right)$) and

$$A = \varepsilon_m - 1, \quad B = \varepsilon_m + 1, \quad A_0 = \frac{1}{Pr} + \frac{\varepsilon_m}{Pr_\tau}. \tag{20}$$

The non-dimensional parameters entering into the problem under consideration are

$Re = \dfrac{\bar{h}\bar{\rho}\bar{u}_r}{\bar{\mu}}$ (Reynolds number), $\qquad Ec = \dfrac{\bar{u}_r^2}{\bar{c}_p(\bar{T}_u - \bar{T}_l)}$ (Eckert number),

$\theta = \dfrac{\bar{T}_l}{\bar{T}_u - \bar{T}_l}$ (Temperature parameter), $\qquad Pr = \dfrac{\bar{c}_p\bar{\mu}}{\bar{k}}$ (Prandtl number),

$$Mn_F = \frac{\overline{\mu}_o \overline{H}_o^2 \overline{K}(\overline{T}_u - \overline{T}_l)}{\overline{\rho}\overline{u}_r^2} \text{ (Ferromagnetic (FHD) parameter),}$$

$$Mn_M = \frac{\overline{\mu}_o^2 \overline{H}_o^2 \overline{h}^2 \overline{\sigma}}{\overline{\mu}} \text{ (Magnetohydrodynamic (MHD) parameter).}$$

The most important parameters entering to the problems of BFD are the two magnetic parameters, Mn_F and Mn_M, defined above. Especially, the Mn_M parameter is the square of the widely known in MHD Hartmann number [31] ~ [33]. Increment of the above mentioned dimensionless parameters, for a specific fluid (ν , σ, ρ , μ_o = const) and for a specific flow problem ($\overline{h}$ =const) means increment of the magnetic field strength induction B_o .

It is worth mentioning here, that when these magnetic parameters $Mn_F = Mn_M = 0$ the problem is a common hydrodynamic channel flow with heat transfer. For a specific Reynolds number and temperature difference, an increase in the values of these magnetic parameters means a corresponding increase in the value of the magnetic field strength, H_0.

For ε_m=0 and Pr_t=1 the system of equations (17) ~ (19), which governs the turbulent flow in the channel, becomes the one that governs the laminar flow in the channel studied in [35].

3.1 Boundary Conditions

For the solution of the system of equations (17) ~ (19), boundary conditions are required for the unknown functions Ψ, J and T. The boundary conditions for Ψ are implemented from (16), since the velocity components are known (fully developed flow at the entrance and no slip conditions on the plates). Considering equations (14) and (16) the value of Ψ at the entrance is calculated to be $\Psi(0, y) = 2y^2 - (4/3)y^3$, ($0 \le y \le 1$).

The dimensionless temperature T at the plates is also easy calculated from (14). It is additionally assumed that in the entrance of the channel T is varying linearly and is given by the expression $T(0, y) = y$.

At the exit of the channel all unknown quantities are assumed to be independent on x ($\partial R / \partial x = 0$, where R stands for Ψ, J or T). Thus, the outflow conditions for all quantities are determined from the interior grid points of the computational domain using second order backward finite differences.

However, in order to solve the vorticity transport equation (18) it is also necessary to determine boundary conditions of the vorticity J and this is not an easy task. For the derivation of boundary conditions of J on the solid surfaces (plates), numerical boundary conditions are constructed, using the stream function Ψ, as described in detail in [35] and [36].

The vorticity at the boundary point (i,m) (see Figure 2), provided that the borders are still (u=v=0), is calculated from the formula.

$$J_{i,m} = -\frac{1}{(\Delta x)^2}\left(\Psi_{i+1,m-1} - 2\Psi_{i,m-1} + \Psi_{i-1,m-1}\right) - \frac{2}{3(\Delta y)^2}\left(\Psi_{i,m-2} - \Psi_{i,m-1}\right) \tag{21}$$

Summarizing the above, the boundary conditions used for the problem under consideration are

Inflow conditions	$(x = 0 , 0 \le y \le 1)$:	$\Psi = 2y^2 - (4/3)y^3$, $J = 8y - 4$, $T = y$,	
Outflow conditions	$(x = L/h , 0 \le y \le 1)$:	$\partial(R)/\partial x = 0$, where R=Ψ, J or T,	(22)
Upper plate	$(y = 1 , 0 \le x \le L/h)$:	$\Psi = 2/3$, J as in (21), $T = 1$,	
Lower plate	$(y = 0 , 0 \le x \le L/h)$:	$\Psi = 0$, J as in (21), $T = 0$.	

3.2 Turbulence model

As it is already mentioned, it has been observed that the blood flow becomes turbulent under certain situations, like the presence of stenosis that result to a highly disturbed flow field [37]~[41]. For the biomagnetic (blood) channel flow [34] ~ [36], it has been observed that the application of a magnetic field results also to high disturbances in the flow field. Moreover, the appearing disturbances in biomagnetic fluid flow field are obviously more intense that the analogous appearing for example in stenotic regions, especially in the case of application of strong magnetic fields (high magnetic parameters).

The Re numbers appearing in biomagnetic fluid flow problems are generally low. Hence, in order to study, numerically, the turbulent flow of the problem under consideration the low Reynolds number k-ε turbulence model is employed. This model takes into account the effects of the viscous sub layer. Generally, in the case of the low Reynolds number k-ε turbulence model, extra terms and modified constants have been added to the standard k-ε model, so that this model is also applicable in the low Re ranges. A variety of low Re k-ε turbulence models have been proposed by different researchers. In the present study, the low Re k-ε turbulence model proposed in [44] is used.

Thus, the rate of turbulent dissipation ε and the turbulent kinetic energy k are given by the solution of the system of equations

$$u\frac{\partial k}{\partial x}+v\frac{\partial k}{\partial y}=\frac{\partial}{\partial x}\left\{\left(\nu+\frac{\varepsilon_m}{\sigma_k}\right)\frac{\partial k}{\partial x}\right\}+\frac{\partial}{\partial y}\left\{\left(\nu+\frac{\varepsilon_m}{\sigma_k}\right)\frac{\partial k}{\partial y}\right\}+\varepsilon_m\left(\frac{\partial u}{\partial y}\right)^2-\varepsilon+D\,, \tag{23}$$

$$u\frac{\partial \varepsilon}{\partial x}+v\frac{\partial \varepsilon}{\partial y}=\frac{\partial}{\partial x}\left\{\left(\nu+\frac{\varepsilon_m}{\sigma_\varepsilon}\right)\frac{\partial \varepsilon}{\partial x}+\frac{\partial}{\partial y}\left\{\left(\nu+\frac{\varepsilon_m}{\sigma_\varepsilon}\right)\frac{\partial \varepsilon}{\partial y}\right\}\right\}+C_1\varepsilon_m f_1\frac{\varepsilon}{k}\left(\frac{\partial u}{\partial y}\right)^2-C_2 f_2\frac{\varepsilon^2}{k}+E\,. \tag{24}$$

The eddy cinematic viscosity ε_m is given by the following relation

$$\varepsilon_m=C_\mu f_\mu\frac{k^2}{\varepsilon} \tag{25}$$

In the above relations

$$C_1=1.55\,,\ f_1=1.0\,,\ C_2=2.0\,,\ f_2=1.0-0.3\exp\left(-R_t^2\right),\ C_\mu=0.09\,,\ f_\mu=\exp\left(\frac{-2.5}{1+R_t/50}\right),\ R_t=\frac{k^2}{\nu\varepsilon}\,,$$

$$\sigma_k=1.0\,,\ \sigma_\varepsilon=1.3\,,\ D=-2\nu\left(\frac{\partial\sqrt{k}}{\partial y}\right)^2,\ E=2\nu\varepsilon_m\left(\frac{\partial^2 u}{\partial y^2}\right)^2.$$

The boundary conditions for the above system of equations are:

$$\begin{aligned}&\text{Inflow conditions} && (x=0\,,0\le y\le 1) &&: \ \varepsilon=k=0\\ &\text{Outflow conditions} && (x=L/h\,,0\le y\le 1) &&: \ \partial\varepsilon/\partial x=\partial k/\partial x=0\end{aligned} \tag{26}$$

Upper plate ($y=1, 0\le x\le L/h$) and Lower plate ($y=0\,,0\le x\le L/h$) : ε = k = 0.

For the turbulent-Prandtl number $\Pr_t$ several expressions have been proposed. In most cases the turbulent-Prandtl number is considered constant. In this study a modification of the Kays and Crawford's model is used [45], [46]. The $\Pr_t$ is given by the expression:

$$\Pr_t = 1/\left\{ \frac{1}{2\Pr_{t_\infty}} + 0.3\mathrm{Pe}_t\sqrt{\frac{1}{\Pr_{t_\infty}}} - (0.3\mathrm{Pe}_t)^2\left[1-\exp\left(-\frac{1}{0.3\mathrm{Pe}_t\sqrt{\Pr_{t_\infty}}}\right)\right]\right\}, \quad (27)$$

where Pe_t is the turbulent Péclet number, given by the relation $\mathrm{Pe}_t = \Pr\varepsilon_m$, and $\Pr_{t_\infty}$ is the value of turbulent-Prandtl number far from the wall [45].

4. Numerical method

The physical problem under consideration, is described by the system of equations (17) ~ (19), (23) ~(24) subject to the boundary conditions (22) and (26) for the unknown quantities Ψ, J, T, k and ε. The quantities ε_m and $\Pr_t$ are evaluated from equations (25) and (27), respectively. This system is coupled and non-linear and an iterative procedure is developed and applied for its numerical solution.

In order to solve, numerically, the system of equations (17)~(19) subject to the boundary conditions (22), an efficient and robust technique has been used, similar to the one used and described in detail in [35] and [36]. The aim of the numerical technique used, for these equations, is to force the coefficients matrices of the unknowns to become diagonally dominant, so as the corresponding equations (18) and (19) will be amenable to solution by iterative methods (i.e. S.O.R or L.L.I.M.).

For the numerical solution of the equations (23)~(24) subject to the boundary conditions (26) a pseudo transient technique is employed. According to this technique the time derivatives of k and ε ($\partial k/\partial t$, $\partial\varepsilon/\partial t$) are added to the corresponding equations (23) and (24). The time plays the role of an iteration parameter and the solution for each time step represents the calculated solution for an iteration step. The solution of (23) and (24) is finally attained by calculating the steady state. The general philosophy of this technique is also demonstrated in [34].

For the solution of the whole system (17)~(19), (23)~(24) an iterative scheme is developed using the above mentioned numerical techniques.

The steps of this iterative numerical scheme are:

- Give initial guesses for Ψ, J and T for the interior points of the computational domain and the boundary conditions.
- Calculate a new estimation for Ψ by solving (17) once, considering J known.
- Considering Ψ known construct the boundary conditions for J using (21).
- Calculate a new estimation for J by solving (18) using the L.L.I.M., considering Ψ, T known.
- Considering now Ψ and J known, calculate a new estimation for T using the L.L.I.M. for (19).
- Calculate a new estimation for k and ε by solving (23) and (24)
- Calculate ε_m and Pr_t from (25) and (27), respectively.
- Compare the new estimations of Ψ, J and T with the old ones. If the criterion of convergence is not satisfied set the new estimations as old and return to the second step.

The criterion of convergence used is

$$\frac{1}{MN}\sum_{i=1}^{M}\sum_{j=1}^{N}\left|F_{i,j}^{n+1}-F_{i,j}^{n}\right|<e$$

where, M and N are the number of grid points towards the x and y direction, respectively, with step size Δx and Δy. $F_{i,j}^{n}$ is an estimation of an unknown function F (Ψ, J or T) at the grid point (i,j), at the n iteration. For the problem under consideration e was taken $e=5\times10^{-5}$.

5. Results

For the numerical solution it is necessary to assign values in the dimensionless parameters entering into the problem under consideration. For these values, in order to be realistic, a similar case scenario to the one adopted in [34] and [36] is considered, in which the fluid is the blood ($\overline{\rho} = 1050 \text{Kgr m}^{-3}$, $\overline{\mu} = 3.2\times10^{-3}\text{kgr m}^{-1}\text{ sec}^{-1}$) [49], flows with maximum velocity $\overline{u}_r = 1.22\times10^{-2}\text{m sec}^{-1}$ and the plates are located at distance $\overline{h} = 5.0\times10^{-2}\text{m}$. In this case the Reynolds number, Re, is equal to 200. The temperature of the plates is $\overline{T}_u = 42\ ^{o}\text{C}$ and $\overline{T}_l = 10.5\ ^{o}\text{C}$. For these values of plate temperatures the temperature parameter θ is equal to 9.

As far as the electrical conductivity of blood for a stationary state is concerned, it was measured to be $\overline{\sigma} = 0.7\text{ s m}^{-1}$ [30]. The electrical conductivity of flowing blood is always greater than that of the stationary. The increment for medium shear rates is about 10% and increases with the increment of the hematocrit [28]. In the present study the electrical conductivity of blood is assumed, for simplicity, temperature independent and equal to 0.8 s m^{-1}.

Although the viscosity $\overline{\mu}$, the specific heat under constant pressure $\overline{c}_p$ and the thermal conductivity $\overline{k}$ of any fluid, and hence of the blood, are temperature dependent, Prandtl number can be considered constant. Thus, for the temperature range considered in this problem, the value of $\overline{c}_p$ and $\overline{k}$ is equal to 14.286 Joule $\text{kgr}^{-1}\ ^{o}\text{K}^{-1}$ and 1.832×10^{-3} Joule $\text{m}^{-1}\text{ sec}^{-1}\ ^{o}\text{K}^{-1}$, respectively [50], and hence it can be considered that Pr=25. For these values of the parameters the Eckert number is Ec=3.30×10^{-7}.

The magnetic parameter Mn_F can be written as

$$Mn_F = \frac{\overline{\mu}_o \overline{H}_o^2 \overline{K}(\overline{T}_u - \overline{T}_l)}{\overline{\rho}\overline{u}_r^2} = \frac{\overline{\mu}_o \overline{H}_o \overline{K} \overline{H}_o (\overline{T}_u - \overline{T}_l)}{\overline{\rho}\overline{u}_r^2} = \frac{\overline{B}\overline{M}}{\overline{\rho}\overline{u}_r^2}, \qquad (28)$$

where $\overline{B}$ and $\overline{M}$ are the magnetic induction and the magnetization, respectively. For magnetic field equal to 10 Tesla, the blood has reached magnetization of 40A m^{-1} [27].

From the definition of the Reynolds number it is also obtained that $\overline{u}_r = \overline{\mu}\,\text{Re}\,\overline{h}^{-1}\overline{\rho}^{-1}$ and substitution of this relation to (28) gives

$$Mn_F = \frac{\overline{B}\overline{M}\overline{h}^2\overline{\rho}}{\overline{\mu}^2\,\text{Re}^2} \qquad (29)$$

From equation (29) and from the definition of the magnetic parameter Mn_M it is obtained that

$$\frac{Mn_F}{Mn_M} = \frac{\bar{\rho}\bar{M}}{\bar{\mu}\bar{B}\bar{\sigma}\,Re^2} \approx \frac{2.051\times 10^6}{Re^2} \tag{30}$$

Thus, for the problem under consideration the Mn_F is determined from equation (29) and the corresponding Mn_M is determined by (30). Representative values of the two magnetic parameters for Re=200 are given in Table I. As it can been seen from this table the corresponding to 10 Tesla magnetic field values of the magnetic parameters are $Mn_F \approx 2563.48$ and $Mn_M \approx 62.5$.

The dimensionless length of the channel was chosen to be 13, the magnetic field is applied between the points x_1=3.5, x_2=8 and the parameter a_1=a_2=4 (see Fig 1). The present results were obtained for a number of grid points equal to $M\times N = 450\times 35$ at the x and y direction, respectively, i.e. 16,200 grid points. Calculations were made also for 320×30, i.e. 9,600 grid points and 520×45, i.e. 23,400 and no significant differences were found.

It is worth mentioning here, that for ε_m=0 and Pr_t=1, the system of equations (17)~(19) that governs the turbulent flow in the channel, becomes the one that governs the laminar flow studied in [35]. Thus, the physical problem of the laminar flow investigated in [35] is actually a special case of the problem investigated in the present study. Consequently, results are also obtained for the case of laminar flow by setting ε_m=0, Pr_t=1, the dimensionless length of the channel equal to 18, the number of grid points 730×35 i.e. 25,550 and for the same values of the rest of the dimensionless parameters entering into the problem under consideration (Mn_F, Mn_M, Re, Pr, etc.). These results are similar to those obtained in [35].

Figs. 3 and 4 show the stream function contours for the values of the above mentioned parameters for various magnetic numbers for turbulent (Fig. 3) and laminar (Fig. 4) flow, respectively. The dimensionless distance x is indicated on the axis at the bottom of the figures and the vertical dashed lines indicate the entrance, the exit of the duct and the positions x_1 and x_2 between of which the magnetic field is applied (see Fig. 1). The values of the magnetic parameters are increased (namely the applied magnetic field) from the top to the bottom of each figure. It is observed, from both figures, that the primary effect of the applied magnetic field, is the formation of two vortices at the area of the points x_1 and x_2. The first vortex rotates counter clockwise, whereas the second one clockwise. From direct comparison of the two figures it is easily apparent that the effect of the magnetic field in the case of the laminar flow is much stronger than that of the turbulent one. The two vortices in the case of the turbulent flow (Fig. 3) are formed for moderate and relatively high magnetic fields and only in the area of the points x_1 and x_2. For relatively weak magnetic fields only a disturbance is raced at the points x_1, x_2. In the laminar case (Fig. 4) other vortices are formed between the points x_1, x_2 and downstream the x_2 point. In this case the aforementioned vortices are arising even for relatively weak magnetic fields. The length of the duct is considered smaller in the turbulent case due to the fact of the reduced effect on the flow. Results analogous to the laminar case have been extensively discussed in [35].

The vorticity function contours for the turbulent and laminar flow are shown in Figs 5 and 6, respectively, for the aforementioned values of the parameters. It should be remarked that in the absence of the magnetic field (Mn_M=Mn_F=0) the stream function as well as the vorticity function contours are straight lines.

The profiles of the dimensionless velocity component u, for the turbulent flow, along specific locations in the channel are shown in Fig. 7. The profile at x=0 is the laminar one imposed to the entrance and from the profiles at x= 3.5 and 8 it is obtained that the first vortex rotates counter clockwise, whereas the second one clockwise. The flow field at the x=5, between the two vortices, does not seem to be disturbed so significantly as in the corresponding laminar case pictured in Fig. 4. Finally, the u velocity profile at the exit (x=13) is reverted to the characteristic profile for the turbulent flow. This last profile (at x=13) is pictured in conjunction with the laminar profile at the entrance.

Fig 8 shows the dimensionless temperature contours for the greatest and the smallest values of the magnetic parameters considered in the previous cases. For each magnetic parameter, two temperature contours are shown, one corresponding to the laminar flow and the other to the turbulent one. It is apparent that for the turbulent flow, the effect of the application of the magnetic field on the temperature, irrespective its strength is almost insignificant and is restricted close to the points x_1 and x_2. On the contrary, the effect of the magnetic field on the temperature field is significant for the laminar flow and the disturbances are propagating all over the flow field even very far downstream the x_2 point (x=18). Detailed discussion for the temperature field of the laminar flow has been given in [35].

The most important flow and heat transfer characteristics are the local skin friction coefficient and the local rate of heat transfer coefficient expressed by the Nusselt number. These quantities can be defined by the following relations

$$C_f = \frac{2\bar{\tau}_l}{\bar{\rho}\bar{u}_r^2} \qquad \text{and} \qquad Nu = \frac{\dot{\bar{q}}\bar{h}}{\bar{k}(\bar{T}_u - \bar{T}_l)} \tag{31}$$

where $\bar{\tau}_l = \bar{\mu}(\partial\bar{u}/\partial\bar{y})\big|_{\bar{y}=0 \text{ or } \bar{h}}$ is the wall shear stress and $\dot{\bar{q}} = -\bar{k}(\partial\bar{T}/\partial\bar{y})\big|_{\bar{y}=0 \text{ or } \bar{h}}$ is the rate of heat flux between the fluid and the plates.

By using (14)~(16), the above mentioned quantities can be written as

$$C_f = \left.\frac{2\Psi''(x,y)}{Re}\right|_{y=0 \text{ or } 1} \qquad \text{and} \qquad Nu = \left.\frac{\partial T}{\partial y}\right|_{y=0 \text{ or } 1} = T'(x,y)\big|_{y=0 \text{ or } 1} \tag{32}$$

where Nu is the Nusselt number, $\Psi''(x,y)\big|_{y=0 \text{ or } 1}$ is the dimensionless wall shear parameter and $T'(x,y)\big|_{y=0 \text{ or } 1}$ is the dimensionless wall heat transfer parameter.

The variation of the dimensionless wall shear parameter, for the turbulent flow, for the lower (y=0) and the upper wall (y=1) are shown in Figs. 9 and 10, for Mn_F=2563.48, 1281.74, 512.69 and for corresponding Mn_M=62.5, 15.62 and 2.5, respectively. For both lower and upper wall and for all the magnetic parameters two major extremum appear in the flow field. The first one is a maximum just after the point x_1(=3), whereas, the second one is a minimum just before the point x_2(=8). It is remarkable that the variation of the dimensionless wall shear parameter (skin friction coefficient) is qualitatively the same irrespectively the plate (lower or upper) and the applied magnetic field (magnetic parameter). For the lower plate also, an increment of the skin friction is observed in the entrance of the channel (0<x<1) due to the development of the turbulent flow since the imposed initial profile is the laminar one. Analogous behavior is observed for the upper plate with a decrement taking place at the entrance. Far downstream the skin friction for both cases, takes the value attained after this variation in the entrance ($x \approx 0.6$). It is also obvious that the increment of the magnetic field strength results to greater variations of these parameters all over the flow field. The important information that can be extracted is the points where the wall shear parameter takes its maximum, minimum and zero values. In the extremum points the wall shear parameter (and consequently the skin friction) is maximized, whereas, is zero in the x points where the skin friction becomes zero. The change of the sign also, denotes anastrophe of the flow. These results may be interesting in the case of creation or reduction of fibrinoid.

Figs 11 and 12 show the variation of the wall shear parameter of the lower and upper plate, respectively. The results, for each wall, are presented for Re=200, Mn_F=2563.48, and Mn_M=62.5 and for the laminar and turbulent flow. From these figures it is apparent that the variation of the lower wall shear parameter for the laminar flow is much greater than that of the turbulent one, especially in the region of the points x_1 and x_2. The interesting result, which can be obtained from the magnification on the right-hand side of the Fig. 12, is that the skin friction for the turbulent flow has greater values than that of the laminar one along the lower plate, except the region of the two points x_1 and x_2. At the region of the point x_1, and specifically from $x \approx 2.25$, the skin friction for the laminar flow begins to increase rapidly and overcomes the skin friction of the turbulent flow until the point $x \approx 4$ where a rapid decrement takes place and the skin friction of the laminar flow becomes again less than that of the turbulent one. At the region of the point x_2, and from $x \approx 7.25$, the skin friction for the laminar flow begins to decrease rapidly and become much less than the skin friction of the turbulent flow until the point $x \approx 8.25$, where a rapid increment takes place and the skin friction of the laminar flow becomes again greater than that of the turbulent one. At the point $x \approx 9.75$, the laminar skin friction becomes again lower than the corresponding turbulent one.

An analogous behavior is observed for the skin friction of the upper wall pictured in Fig. 12. In that case, and from the magnification on the right-hand side of the Fig. 12, it is concluded that the skin friction for the turbulent flow is smaller than that of the laminar one for approximately $0<x\leq 4.25$ and for $x\geq 8.25$. In the region of $4.25<x<8.25$ the turbulent skin friction becomes greater than the corresponding laminar one.

Figs. 13 and 14 show the variation of the dimensionless wall heat transfer parameter, for the turbulent flow, for the lower and upper plate, respectively and for three different values of the magnetic parameters Mn_F=2563.48, Mn_F=1281.74 and Mn_F=512.69 with corresponding Mn_M=62.5, Mn_M=15.62 and Mn_M=2.5. For both plates, a rapid increment of the heat transfer takes place in the entry region of the plates justified from the development to the turbulent flow. For both plates also, the variation of the heat transfer parameter is made almost in the same way for the three different values of the magnetic parameters and two maximums are observed at the points x_1 and x_2.

For the lower plate (Fig. 13) the global maximum, for all the aforementioned values of the magnetic parameters, is attained at the x_1 point. Another disturbance in the dimensionless wall heat transfer parameter resulting in a second maximum, but much smaller than the previous one, appears in the point x_2. For the upper plate analogous behavior for the dimensionless wall heat transfer parameter is observed, as it can be concluded from the Fig. 14, with the global maximum appearing this time at the x_2 point. This behaviour of the dimensionless wall heat transfer parameter for the lower and upper plate is justified by the presence and the way of rotation of the vortices at the regions of the points x_1 and x_2 (Fig. 3). Finally, downstream the point x_2 the value of $T'(x,0)$ or $T'(x,1)$ (Figs. 13 and 14) reach their prior values attained just after the entrance of the channel once the turbulent flow has been developed.

The dimensionless wall heat transfer parameter for Re=200, Mn_F=2563.48 and Mn_M=62.50 for the laminar in conjunction with the turbulent flow is given in Fig. 15 for the lower and in Fig. 16 for the upper plate, respectively. It can be generally concluded that the variations of the heat transfer parameter for both walls and for the laminar flow, are much more intended and complicated than those of the turbulent one. From Fig. 15 it is apparent that the heat transfer of the lower wall, is greater in the turbulent flow than the laminar one in the region $0<x<12$ with an exception in the region $2.25<x<3$, where a rapid increment takes place for the laminar flow and two other picks occurring at $x \approx 4.5$ and 7.5. At approximately x=12 another rapid increment of the dimensionless wall heat transfer parameter for the laminar flow, takes place and for $x>13$ this parameter takes much greater values than the corresponding in the turbulent one. This latter behavior is justified because in the laminar flow (Fig. 8) a disturbance is generated in that area and is extended far downstream.

Analogous behavior is observed for the dimensionless wall heat transfer parameter of the upper plate. Namely, the dimensionless wall heat transfer parameter, for the turbulent flow, is greater than that of the laminar one, for $0<x<8.5$, with the exception at $x=7$, where the opposite is true (see the magnification on the right-hand side of Fig. 16). From approximately $x=9$ and downstream, the dimensionless wall heat transfer parameter in the case of laminar flow, rapidly increases and overcomes the corresponding of the turbulent one.

6. Conclusions

In the present study the turbulent biomagnetic fluid flow in a rectangular channel under the action of a localized magnetic field is studied. The fluid is considered to be electrically conducting and for the formulation of the turbulence, the low Reynolds number k-ε turbulence model is adopted. The major apparent effect from the application of the localized magnetic field is the formation of two vortices at the area of the points between of which the magnetic field is applied. From the comparison of the results concerning the velocity and temperature field, between laminar and turbulent flow, it is apparent that the effect of the magnetic field significantly reduces by the presence of turbulence. However, the results concerning the velocity, temperature field, skin friction and rate of heat transfer at the walls of the channel, indicate that for the case of turbulent flow, the effect of the magnetic field remains significant. Moreover, in certain areas in the channel, the skin friction and the rate of heat transfer are greater in the case of turbulent flow than that calculated in the case of the laminar one. The above mentioned results indicate that the application of a magnetic field, in the flow of a biomagnetic fluid should be further studied for possible useful medical and engineering applications.

References

[1] U. Häfeli, Magnetism in Medicine, in: Andrä, W. Nowak H. (Eds.), Wiley - VCH, New York, 1998

[2] P.A. Voltairas, D.I. Fotiadis and L.K. Michalis, Journal of Biomechanics 35 (2002) 813–821.

[3] P.A. Voltairas, D.I. Fotiadis, C.V. Massalas, Journal of Magnetism and Magnetic Materials 225 (2001) 248-255.

[4] Ch. Alexiou, A. Schmidt, R. Klein, P. Hulin, Ch. Bergemann, W. Arnold, Journal of Magnetism and Magnetic Materials, 252 (2002) 363–366.

[5] A.S. Lübbe, Ch. Bergemann, J. Brock, D.G. McClure, Journal of Magnetism and Magnetic Materials 194 (1999) 149-155.

[6] J. Plavins, and M. Lauva, Journal of Magnetism and Magnetic Materials, 122 (1993) 349-353.

[7] R. Hiergeist, W. Andrä, N. Buske, R. Hergt, I. Hilger, U. Richter, W. Kaiser, Journal of Magnetism and Magnetic Materials 201 (1999) 420-422.

[8] M. Babincová, P. Čičmanec, V. Altanerová, Č.M Altaner, P. Babineca, Bioelectrochemistry 55 (2002) 17-19.

[9] P. Zheng, Y. Haik, M. Kilani, C.J. Chen, Journal of Magnetism and Magnetic Materials 241 (2002) 292–302.

[10] T. Higashi, A. Yamagishi, T. Takeuchi, N. Kawaguchi, S. Sagawa, S. Onishi, and M. Date, J. Blood 82 (1993) 1328-1334.

[11] C. Gasparovic, and N.A. Matweiyoff, Magnetic Resonance in Medicine 26 (1992) 274-279.

[12] A.N. Shaylgin, S.B. Norina, E.I.Kondorsky, Journal of Magnetism and Magnetic Materials 31 (1983) 555-556.

[13] T. Takeuchi, T. Mizuno, A. Yamagishi, T. Higashi and M. Date, Journal of Magnetism and Magnetic Materials 140-144 (1995) 1462-1463.

[14] T. Higashi, N. Ashida, T. Takeuchi, Physica B (1997) 616-620.

[15] L. Pauling and C.D. Coryell, The magnetic Properties and Structure of Hemoglobin, Oxyhemoglobin and Carbonmonoxy Hemoglobin, In Proceedings of the National Academy of Science, USA, 22 1936, pp. 210-216.

[16] Y. Haik, C.J. Chen and J. Chatterjee, Journal of Visualization 5 (2002) 187-195.

[17] Y. Haik, C.J. Chen and V.M. Pai, Development of bio-magnetic fluid dynamics, In Proceedings of the IX International Symposium on Transport Properties in Thermal Fluids Engineering, Singapore, Pacific Center of Thermal Fluid Engineering, S.H. Winoto, Y.T. Chew, N.E. Wijeysundera, (Eds.), Hawaii, U.S.A., June 25-28, 1996, pp. 121-126.

[18] G.R. Zendehbudi, M.S. Moayeri, Journal of Biomechanics 32 (1999) 959-965.

[19] H.I. Andersson, R. Halden and T. Glomsaker, Journal of Biomechanics 33 (2000) 1257-1262.

[20] V.G. Bashtovoy, B.M. Berkovsky, A.N. Vislovich, Introduction to thermomechanics of magnetic fluids, Hemisphere publishing co., Springer-Verlang, 1988.

[21] B. Berkovski, , V. Bashtovoy, Magnetic fluids and applications handbook, Begell house, New York, 1996.

[22] E. Blums, A. Cebers, M.M. Maiorov, Magnetic Fluids, Walter de Gruyter, Berlin, 1997.

[23] V.E. Fertman, Magnetic fluids guidebook: properties and applications, Hemisphere publishing co., New York, 1990.

[24] R.E. Rosensweig, Ann. Rev. Fluid Mech. 19 (1987) 437-463.

[25] J.L. Neuringer, R.E. Rosensweig, Physics of Fluids 7 (1964) 1927-1937.

[26] R.E. Rosensweig, “Ferrohydrodynamics”, Cambridge University Press, 1985.

[27] Y. Haik, V. Pai, and C.J. Chen, Biomagnetic Fluid Dynamics, In: Fluid Dynamics at Interfaces, W. Shyy and R. Narayanan (Eds.), Cambridge University Press, 1999, pp. 439-452.

[28] R.A. Frewer, Biomedical Engineering (1974) 552-554.

[29] F. Jaspard and M. Nadi, Physiological Measurement 23 (2002) 547-554.

[30] S.Gabriel, R.W. Lau and C. Gabriel, Physics in Medicine and Biology 41 (1996) 2271-2293.

[31] K.R. Cramer and S.I. Pai, Magnetofluid dynamics for engineers and applied physicists, Scripta Publishing Company, Washington D.C., 1973.

[32] W.F. Hughes and F.J. Young, The Electromagnetodynamics of Fluids, John Wiley & Sons, Inc. New York, 1st Ed., 1966.

[33] G.W. Sutton and A. Sherman, Engineering Magnetohydrodynamics, McGraw-Hill, New York, 1965.

[34] E.E. Tzirtzilakis, Physics of Fluids 17 (2005) 077103.

[35] E.E. Tzirtzilakis and V.C. Loukopoulos, Computational Mechanics 36 (2005) 360-374.

[36] V.C. Loukopoulos and E.E. Tzirtzilakis, International Journal of Engineering Science 42 (2004) 571–590.

[37] M. Ohyama, K. Mizushige, H. Ohyama, T. Takahashi, N. Hosomi, S. Ichihara, M. Kohno, International Journal of Cardiovascular Imaging 18 (2002) 119-124.

[38] J.S. Stroud, S.A Berger, D.Saloner, J. of Biomechanical Engineering–Transactions of the ASME 124 (2002) 9-20.

[39] S.S Varghese, S.H. Frankel, Journal of Biomechanical Engineering – Transactions of the ASME 125 (2003) 445-460.

[40] F. Ghalichi, X.Y. Deng, Biorheology 40 (2003) 637-654.

[41] F. Ghalichi, X. Deng, A. Champlain, Y. Douville, M. King and R. Guidoin, Biorheology 35 (1998) 281-294.

[42] H. Matsuki, K. Yamasawa, and K. Murakami, IEEE Transactions on Magnetics 13 (1977) 1143-1145.

[43] N.G. Kafoussias and M.A. Xenos, Acta Mechanica 141 (2000) 201-223.

[44] S. Kotake, K. Hijikata, T. Fusegi, Numerical simulations of heat transfer and fluid flow on a personal computer, Elsevier, Amsterdam, 1993.

[45] B.Weigand, J.R. Ferguson, M.E. Crawford, International Journal of Heat Mass Transfer 40 (1997) 4191-4196.

[46] W.M. Kays and M.E. Crawford, Convective Heat and Mass Transfer, 3rd edn., McGraw-Hill, New York, 1993.

[47] V.C. Loukopoulos, G.A. Katsiaris and G.T. Karahalios, Computer methods in Applied Mechanics and Engineering, 192 (2003) 2993-3003.

[48] S. Patankar, Numerical Heat Transfer and Fluid Flow, Hemisphere Publishing Corporation, 1980.

[49] T. J. Pedley, The fluid mechanics of large blood vessels, Cambridge University Press, 1980.

[50] J.C. Chato, J. Biomechanical Engineering 102 (1980) 110-118.

Caption of Figures

Figure 1. The flow configuration and the magnetic field

Figure 2. Grid points for the calculation of the boundary conditions for J

Figure 3. Stream function contours for various magnetic parameters for turbulent flow

Figure 4. Stream function contours for various magnetic parameters for laminar flow

Figure 5. Vorticity function contours for various magnetic parameters for turbulent flow

Figure 6. Vorticity function contours for various magnetic parameters for laminar flow

Figure 7. Profiles of the dimensionless velocity component u along specific locations in the channel for turbulent flow.

Figure 8. Dimensionless temperature contours for turbulent flow in conjunction with the laminar flow

Figure 9. Variation of the dimensionless wall shear parameter for the lower wall for turbulent flow

Figure 10. Variation of the dimensionless wall shear parameter for the upper wall for turbulent flow

Figure 11. Variation of the dimensionless wall shear parameter of the lower wall for both turbulent and laminar flow. Magnification on the right.

Figure 12. Variation of the dimensionless wall shear parameter of the upper wall for both turbulent and laminar flow. Magnification on the right.

Figure 13. Variation of the dimensionless wall heat transfer parameter, for turbulent flow and for the lower plate

Figure 14. Variation of the dimensionless wall heat transfer parameter, for turbulent flow and for the upper plate

Figure 15. The dimensionless wall heat transfer parameter for laminar in conjunction with turbulent flow for the lower plate

Figure 16. The dimensionless wall heat transfer parameter for laminar in conjunction with turbulent flow for the upper plate

Re = 200		
B (Tesla)	Mn_M	Mn_F
2	2.50	512.69
4	10.00	1025.39
6	22.50	1538.09
8	40.00	2050.78
10	62.50	2563.48

Table I : Various magnetic parameters for Re=200 and for various magnetic field strengths

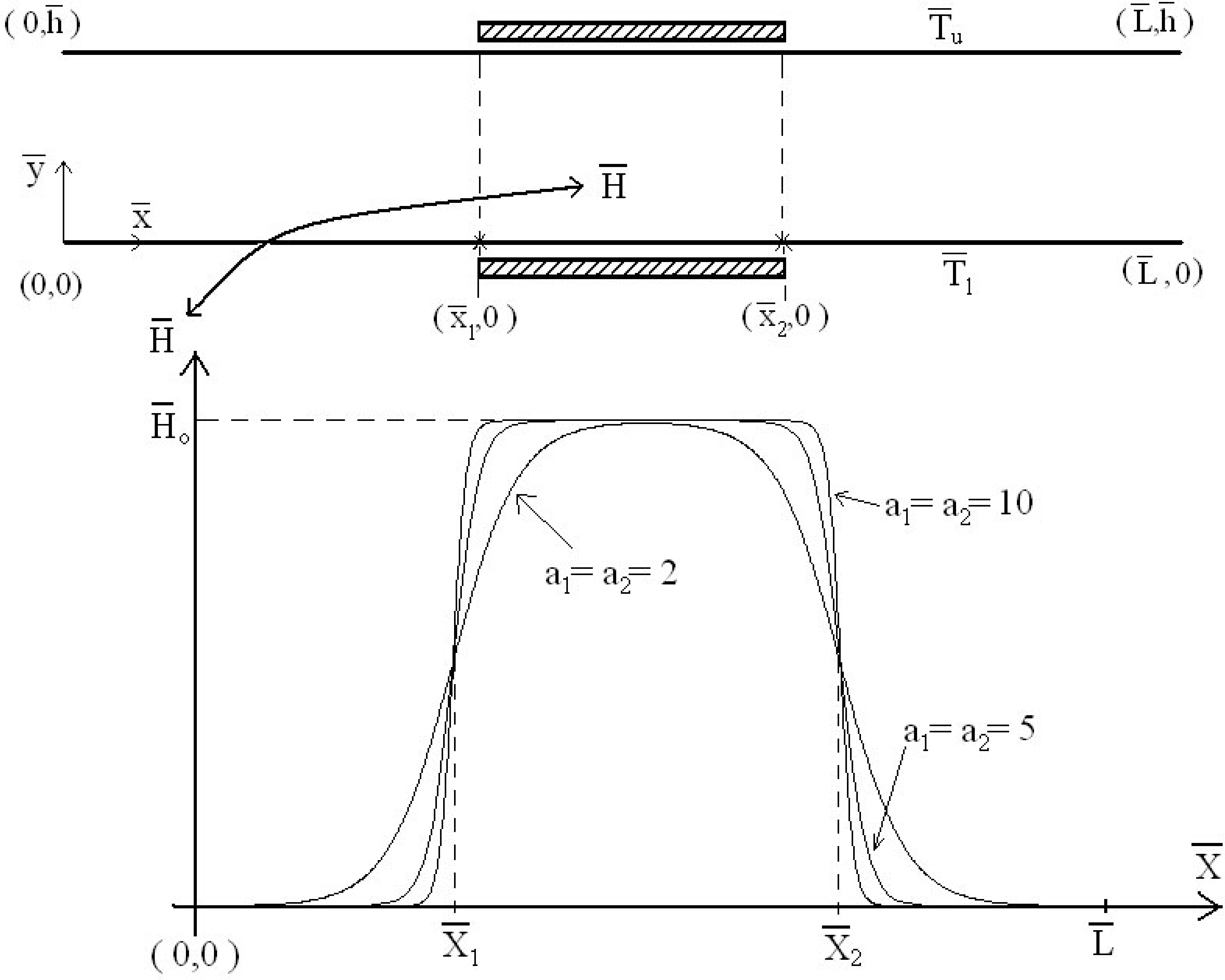

$(0,\overline{h})$
$\overline{T}_u$
$(\overline{L},\overline{h})$
$\overline{y}$
$\overline{x}$
$\overline{H}$
$(0,0)$
$\overline{T}_1$
$(\overline{L},0)$
$(\overline{x}_1,0)$
$(\overline{x}_2,0)$
$\overline{H}$
$\overline{H}_o$
$a_1 = a_2 = 10$
$a_1 = a_2 = 2$
$a_1 = a_2 = 5$
$\overline{X}$
$(0,0)$
$\overline{X}_1$
$\overline{X}_2$
$\overline{L}$

Grid at Boundary

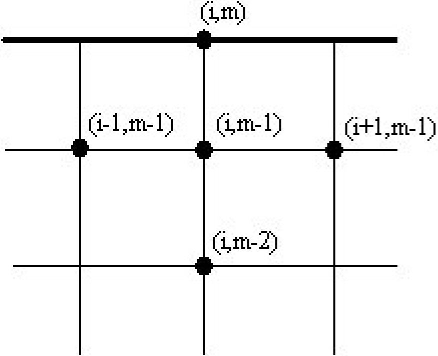

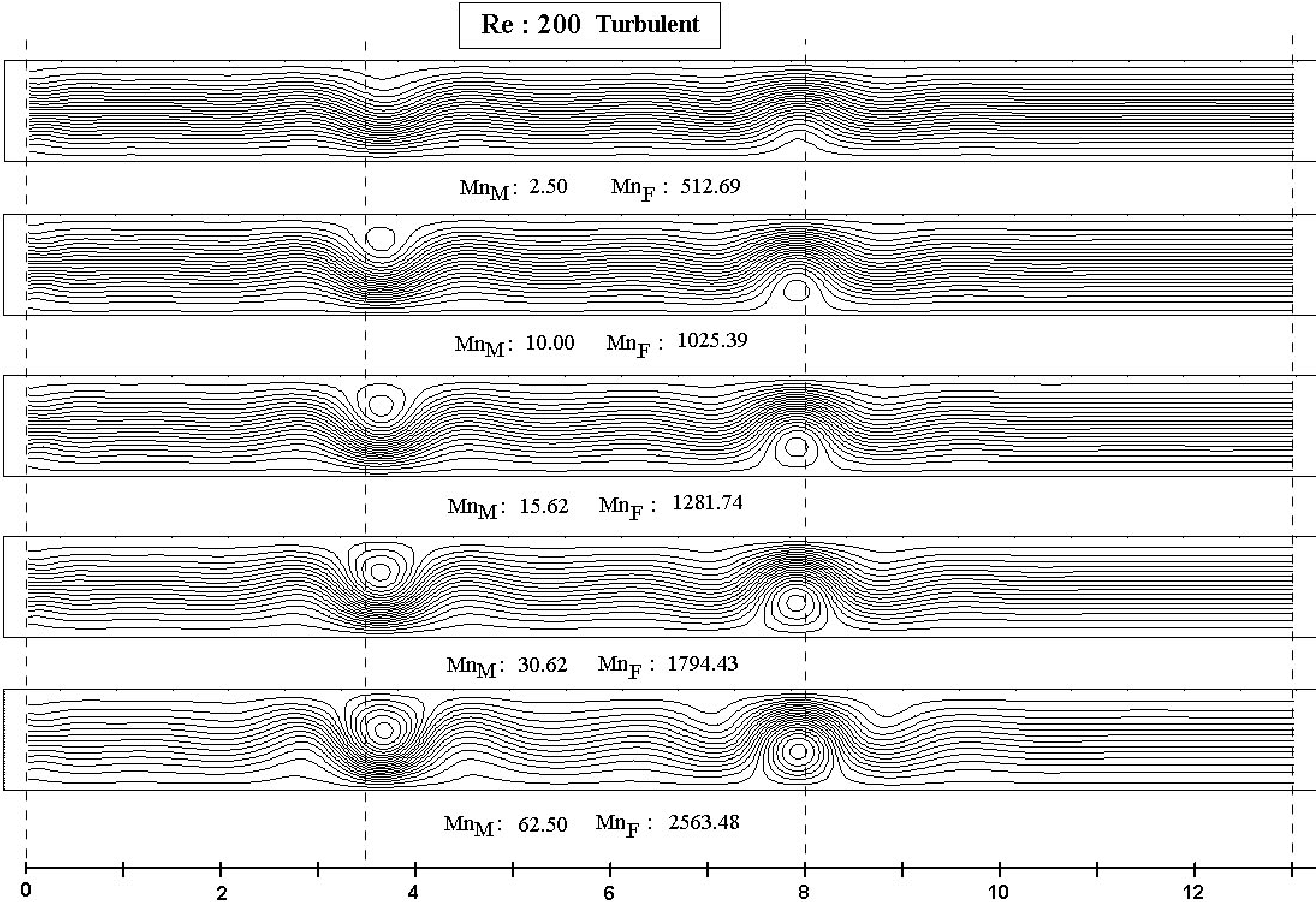

Re : 200 Turbulent
MnM : 2.50 MnF : 512.69
MnM : 10.00 MnF : 1025.39
MnM : 15.62 MnF : 1281.74
MnM : 30.62 MnF : 1794.43
MnM : 62.50 MnF : 2563.48
0
2
4
6
8
10
12

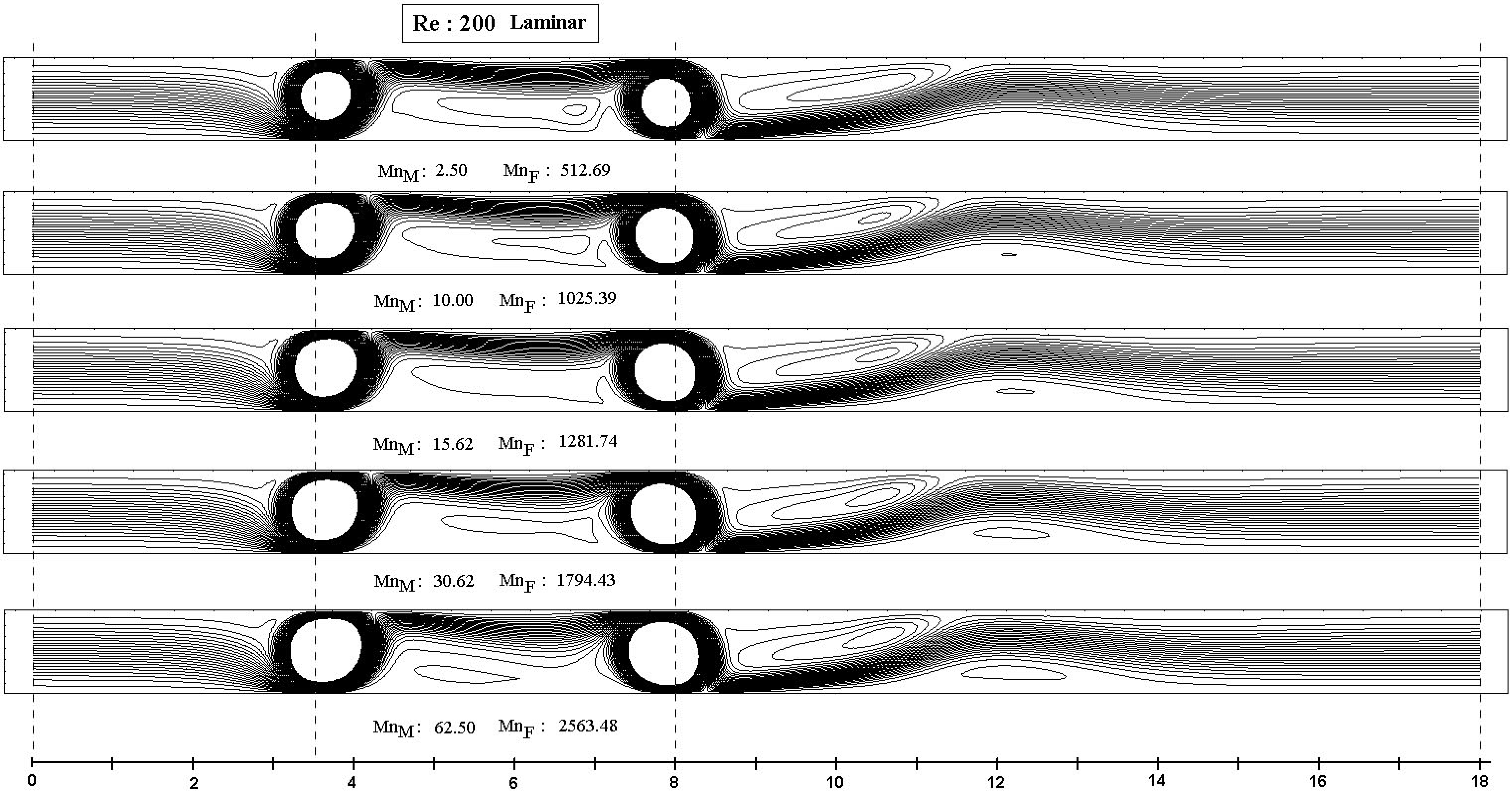

Re : 200 Laminar
Mn_M: 2.50 Mn_F : 512.69
Mn_M: 10.00 Mn_F : 1025.39
Mn_M: 15.62 Mn_F : 1281.74
Mn_M: 30.62 Mn_F : 1794.43
Mn_M: 62.50 Mn_F : 2563.48
0
2
4
6
8
10
12
14
16
18

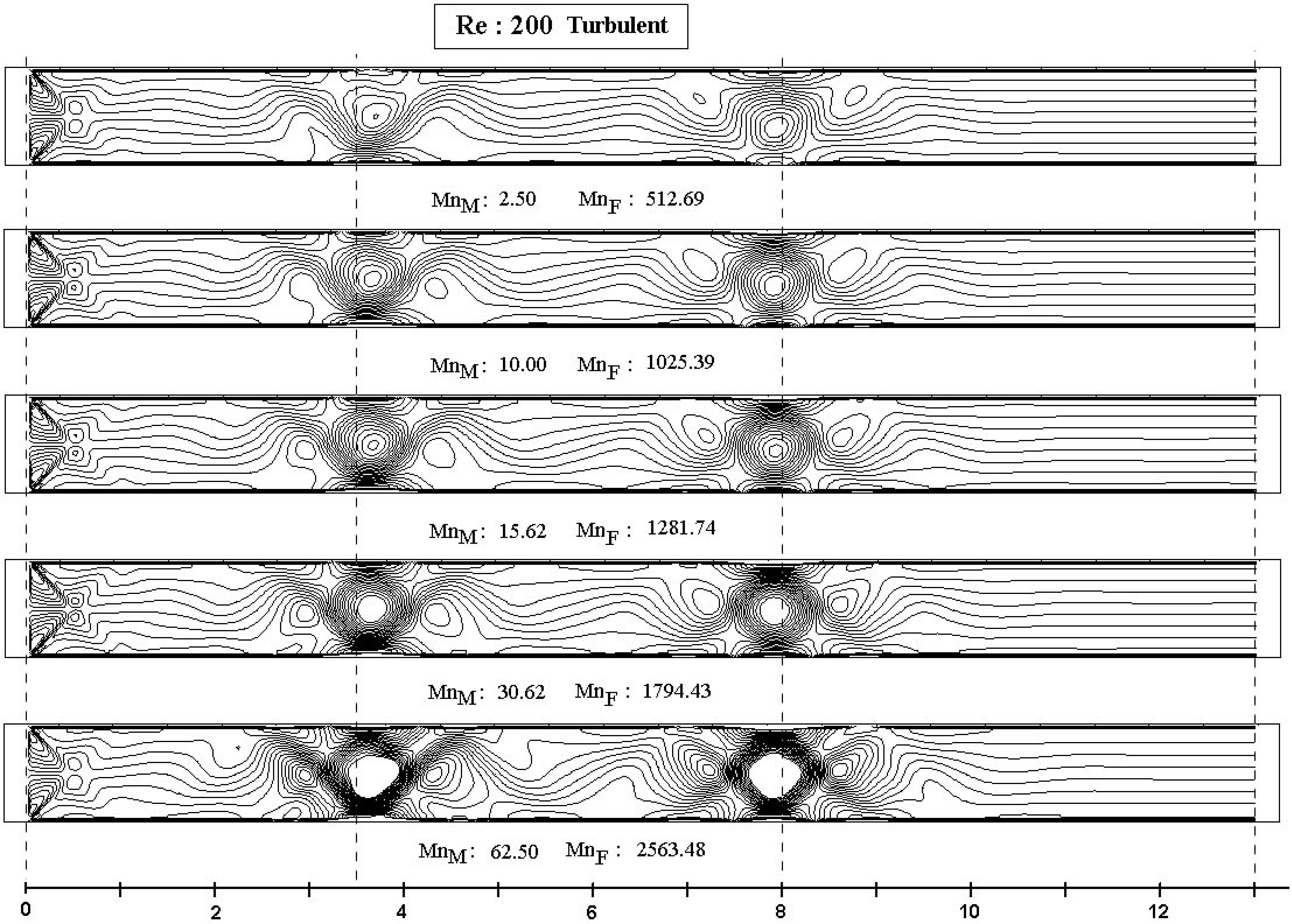

Re : 200 Turbulent
Mn_M: 2.50 Mn_F: 512.69
Mn_M: 10.00 Mn_F: 1025.39
Mn_M: 15.62 Mn_F: 1281.74
Mn_M: 30.62 Mn_F: 1794.43
Mn_M: 62.50 Mn_F: 2563.48
0
2
4
6
8
10
12

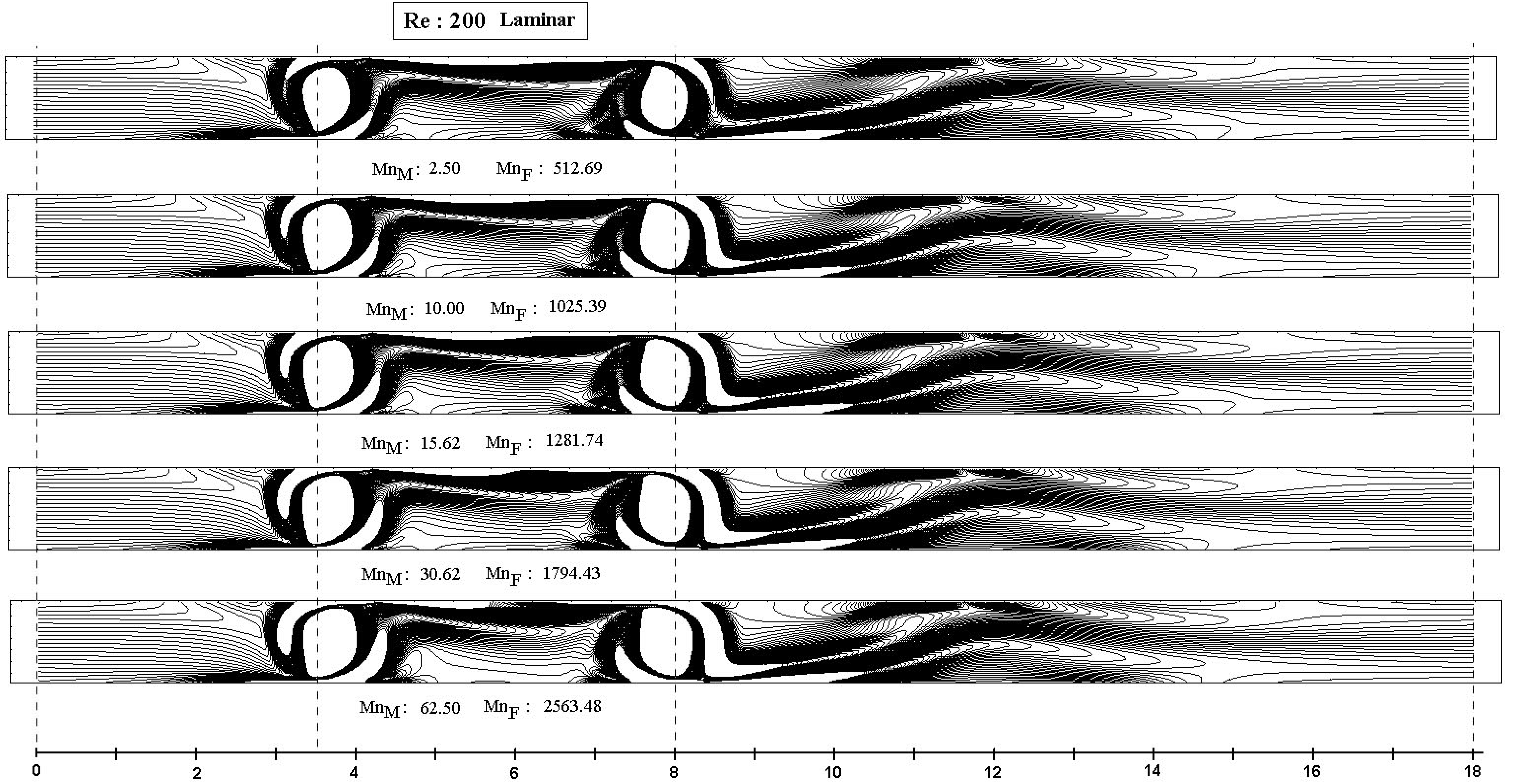
Re : 200 Laminar
Mn_M: 2.50 Mn_F: 512.69
Mn_M: 10.00 Mn_F: 1025.39
Mn_M: 15.62 Mn_F: 1281.74
Mn_M: 30.62 Mn_F: 1794.43
Mn_M: 62.50 Mn_F: 2563.48
0
2
4
6
8
10
12
14
16
18

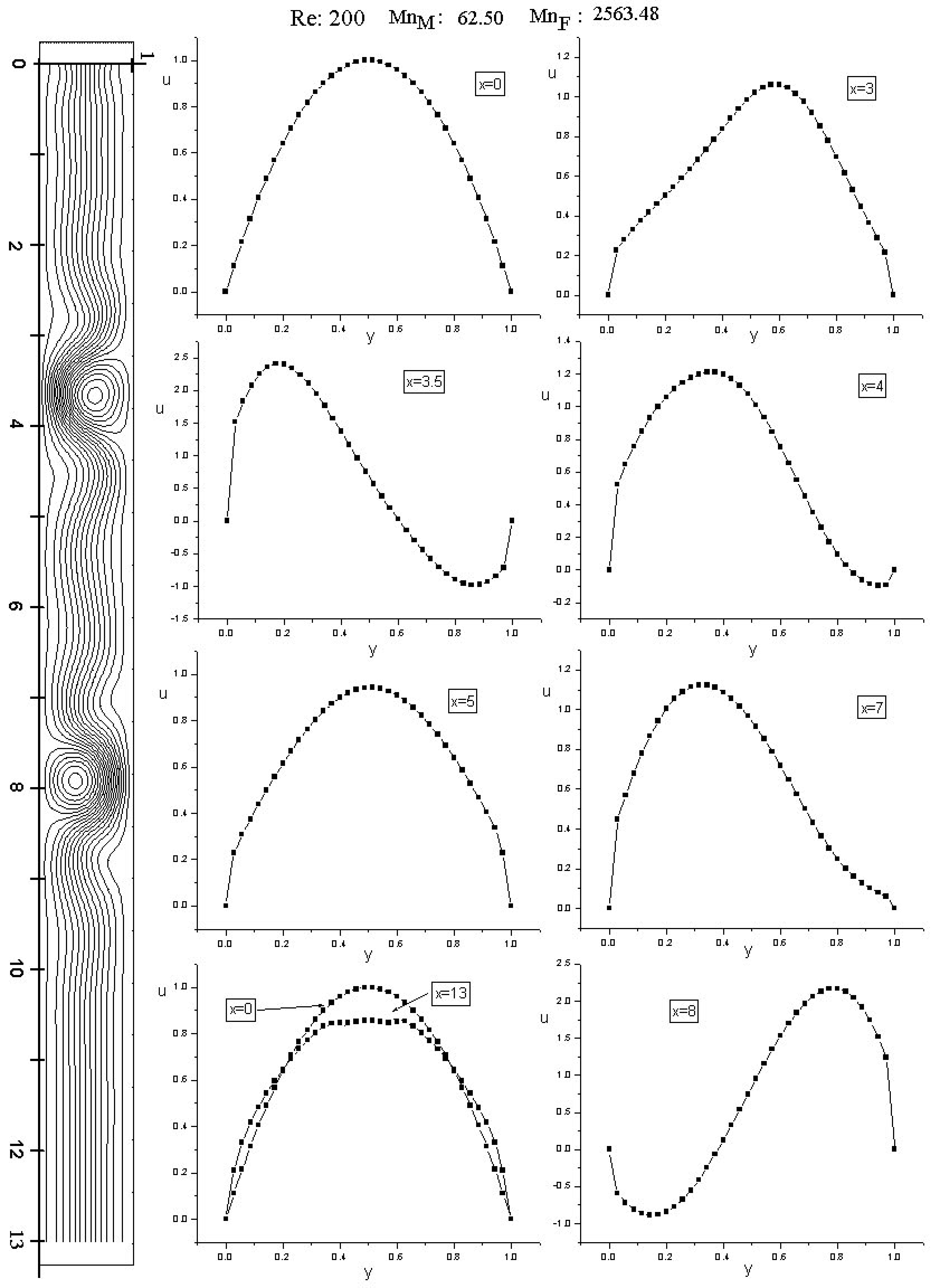

Re: 200 Mn_M: 62.50 Mn_F: 2563.48
x=0
x=3
x=3.5
x=4
x=5
x=7
x=0
x=13
x=8
u
y

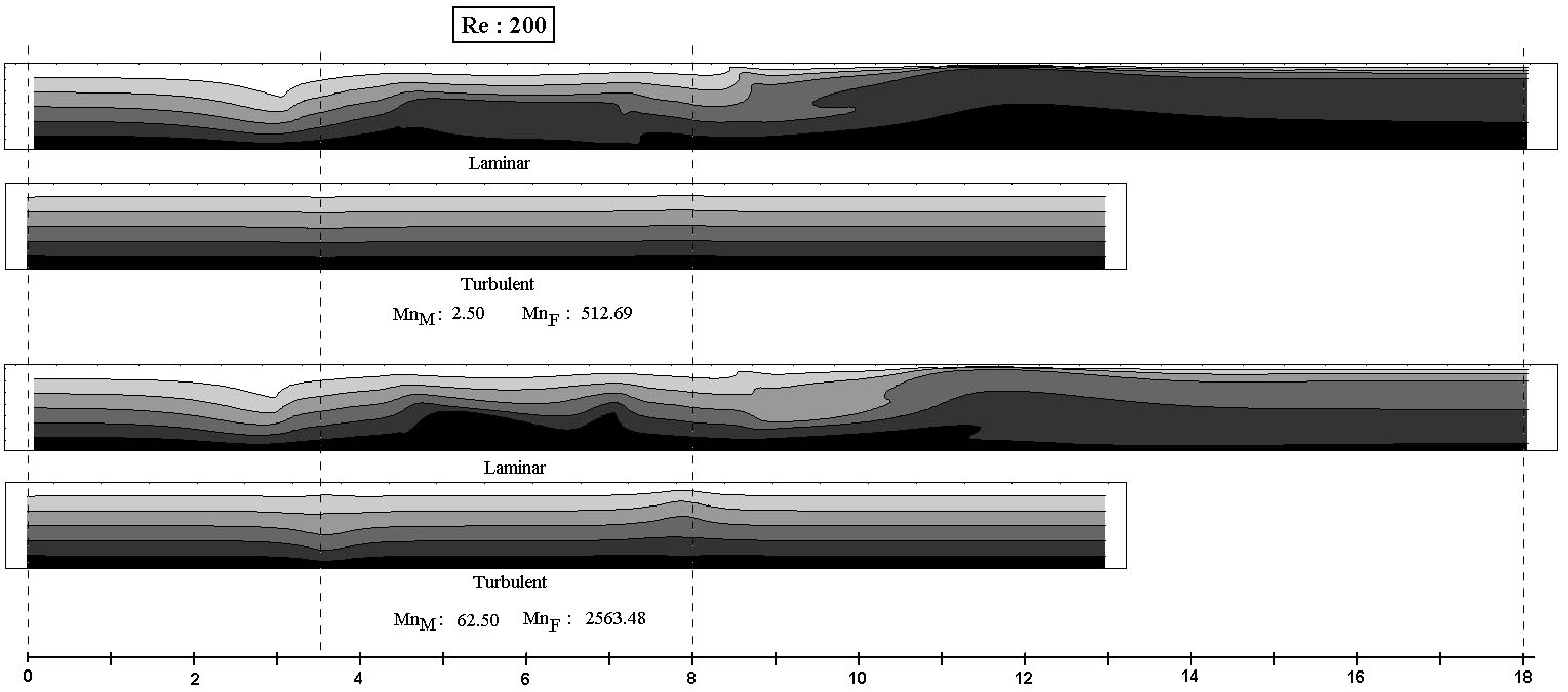

Re : 200
Laminar
Turbulent
Mn_M: 2.50 Mn_F : 512.69
Laminar
Turbulent
Mn_M: 62.50 Mn_F : 2563.48
0
2
4
6
8
10
12
14
16
18

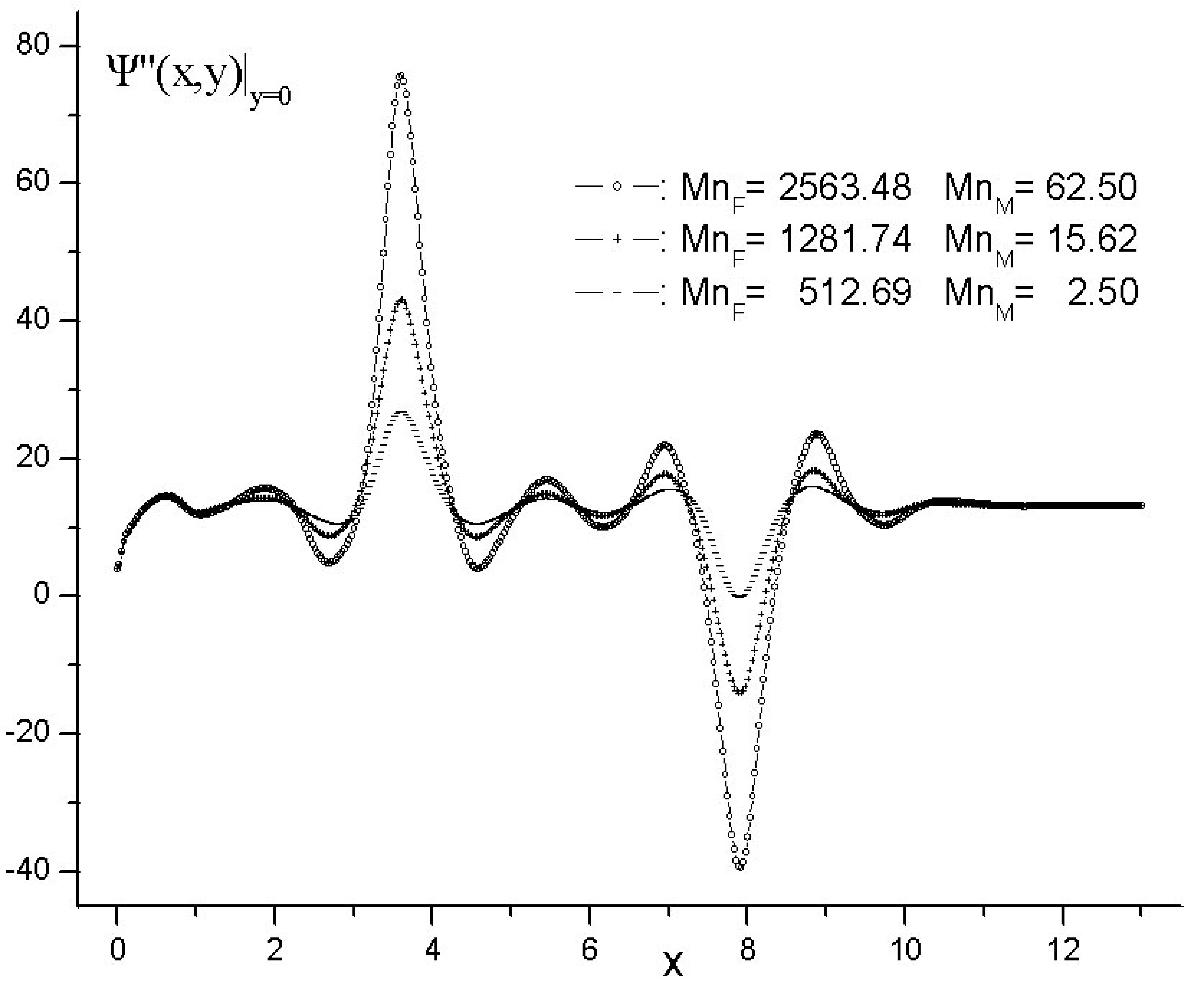

Ψ''(x,y)|y=0
: MnF= 2563.48 MnM= 62.50
: MnF= 1281.74 MnM= 15.62
: MnF= 512.69 MnM= 2.50
80
60
40
20
0
-20
-40
0
2
4
6
8
10
12
x

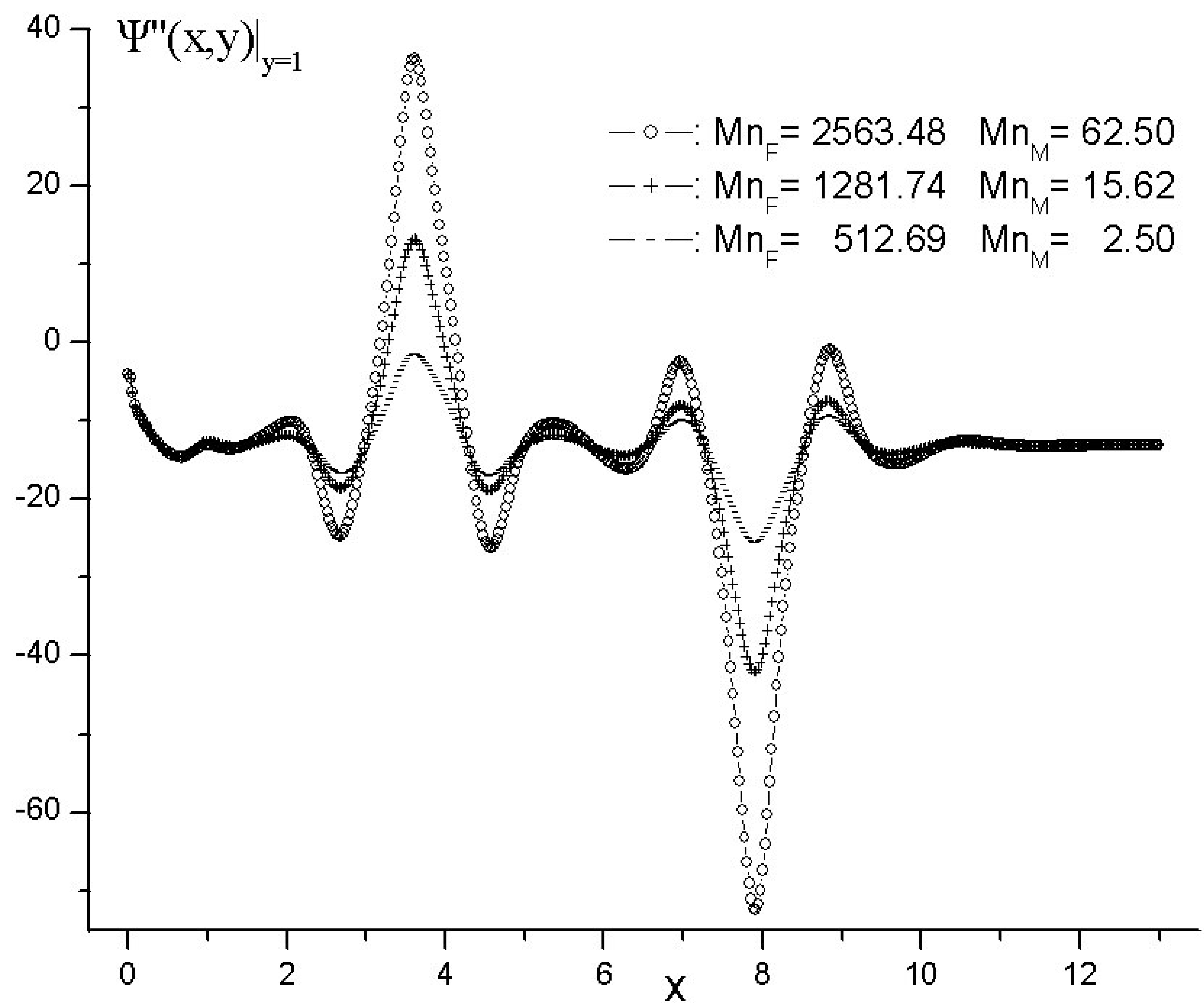

40
20
0
-20
-40
-60
Ψ''(x,y)|y=1
: MnF= 2563.48 MnM= 62.50
: MnF= 1281.74 MnM= 15.62
: MnF= 512.69 MnM= 2.50
0
2
4
6
8
10
12
x

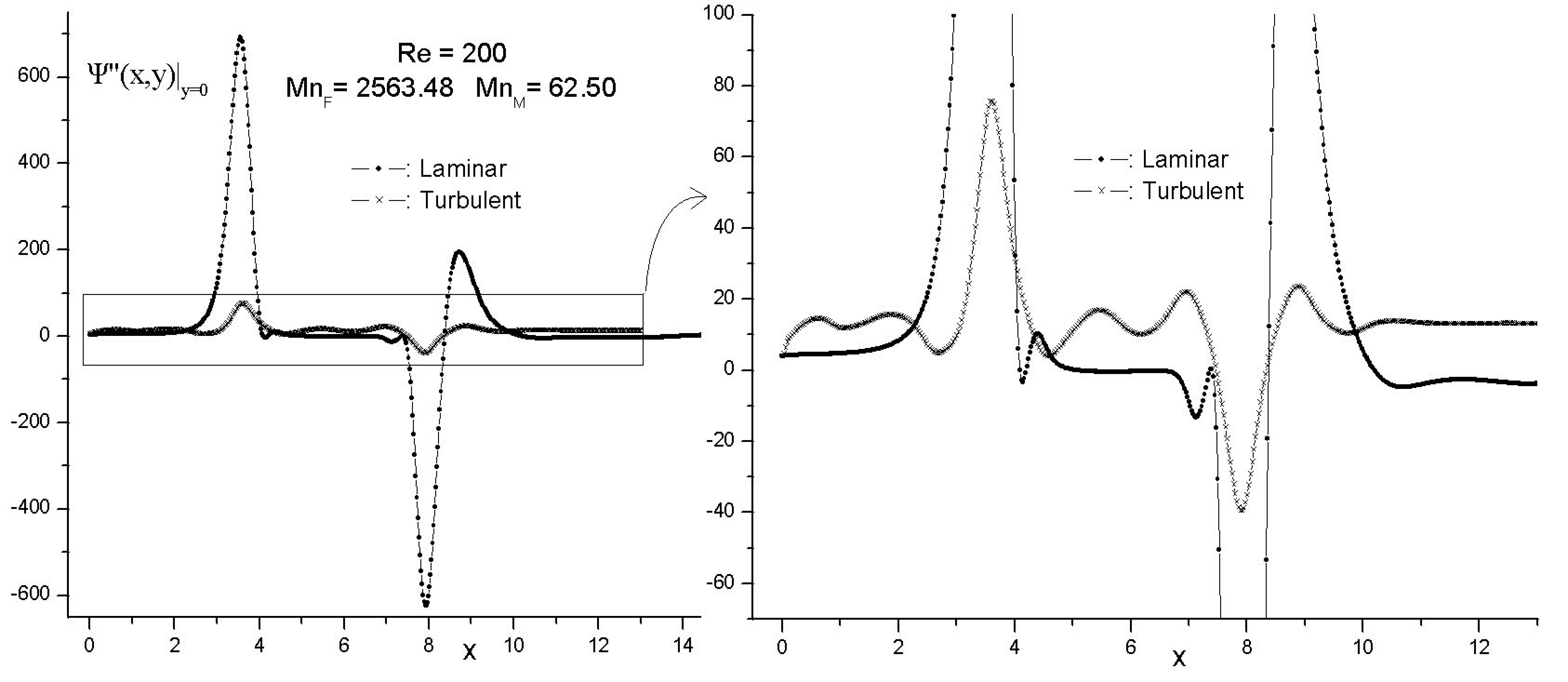

Ψ''(x,y)|y=0
Re = 200
MnF = 2563.48 MnM = 62.50
Laminar
Turbulent
x
Laminar
Turbulent
x

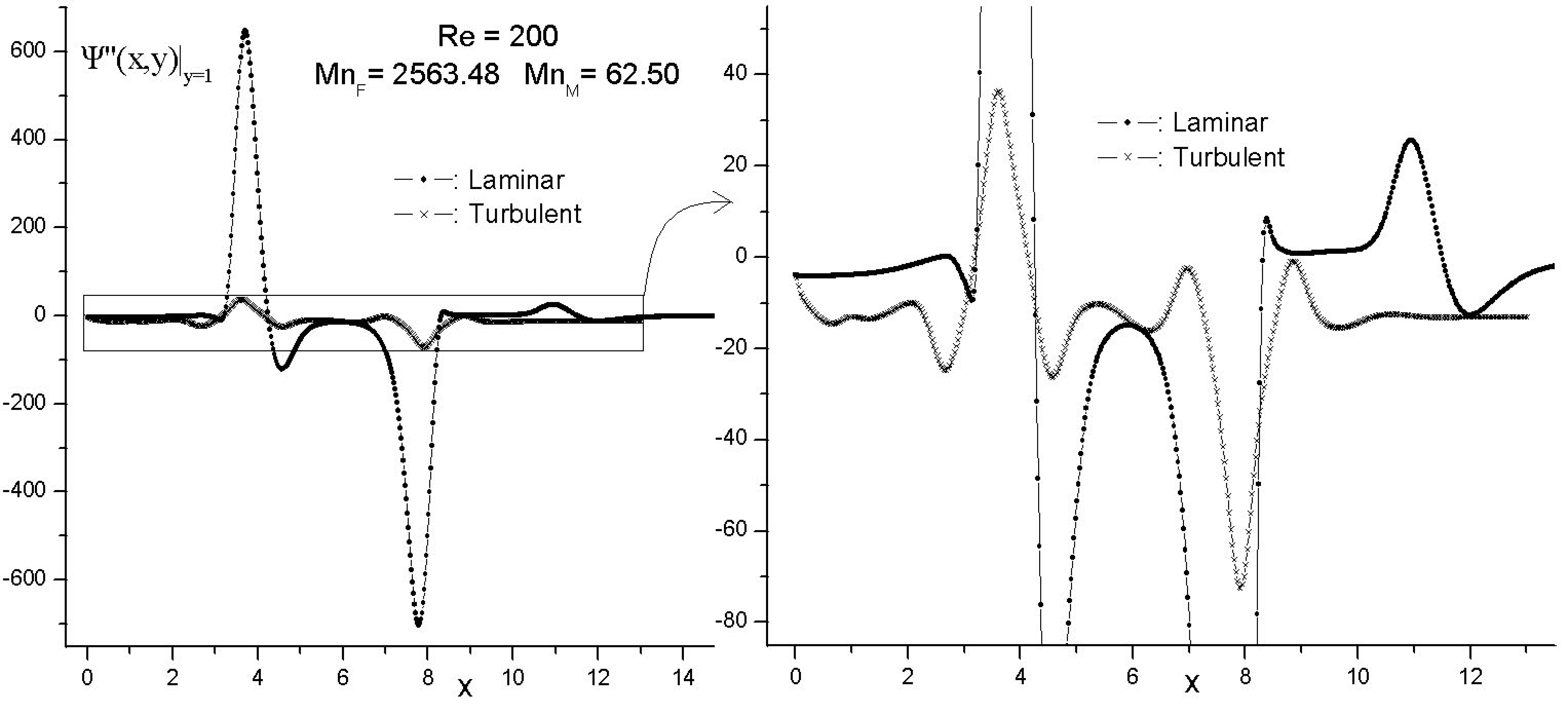

Re = 200
$Mn_F = 2563.48$ $Mn_M = 62.50$
$\Psi''(x,y)|_{y=1}$
Laminar
Turbulent
x
600
400
200
0
-200
-400
-600
0
2
4
6
8
10
12
14
40
20
-20
-40
-60
-80

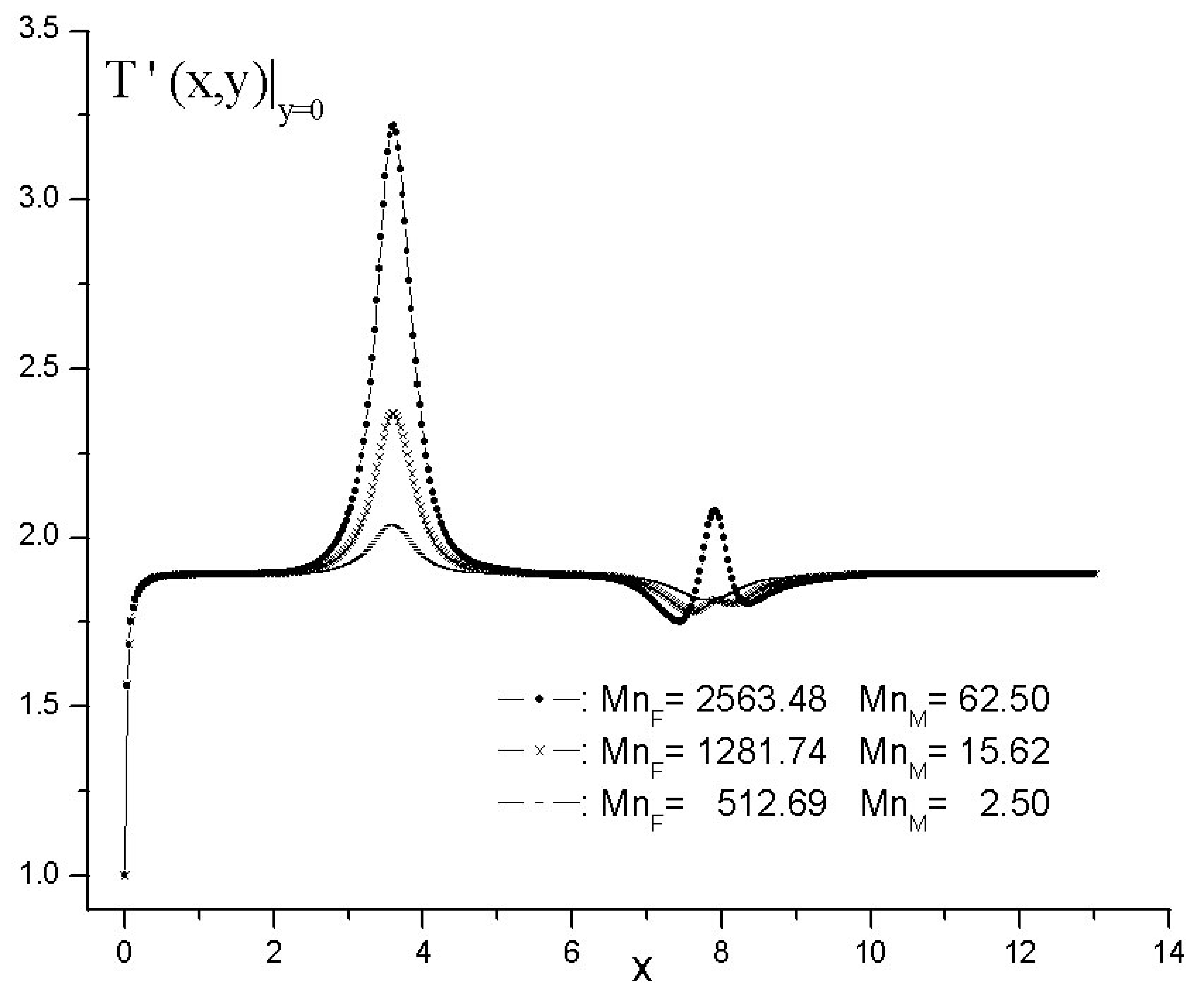
$T'(x,y)|_{y=0}$
3.5
3.0
2.5
2.0
1.5
1.0
0
2
4
6
8
10
12
14
x
: Mn_F= 2563.48 Mn_M= 62.50
: Mn_F= 1281.74 Mn_M= 15.62
: Mn_F= 512.69 Mn_M= 2.50

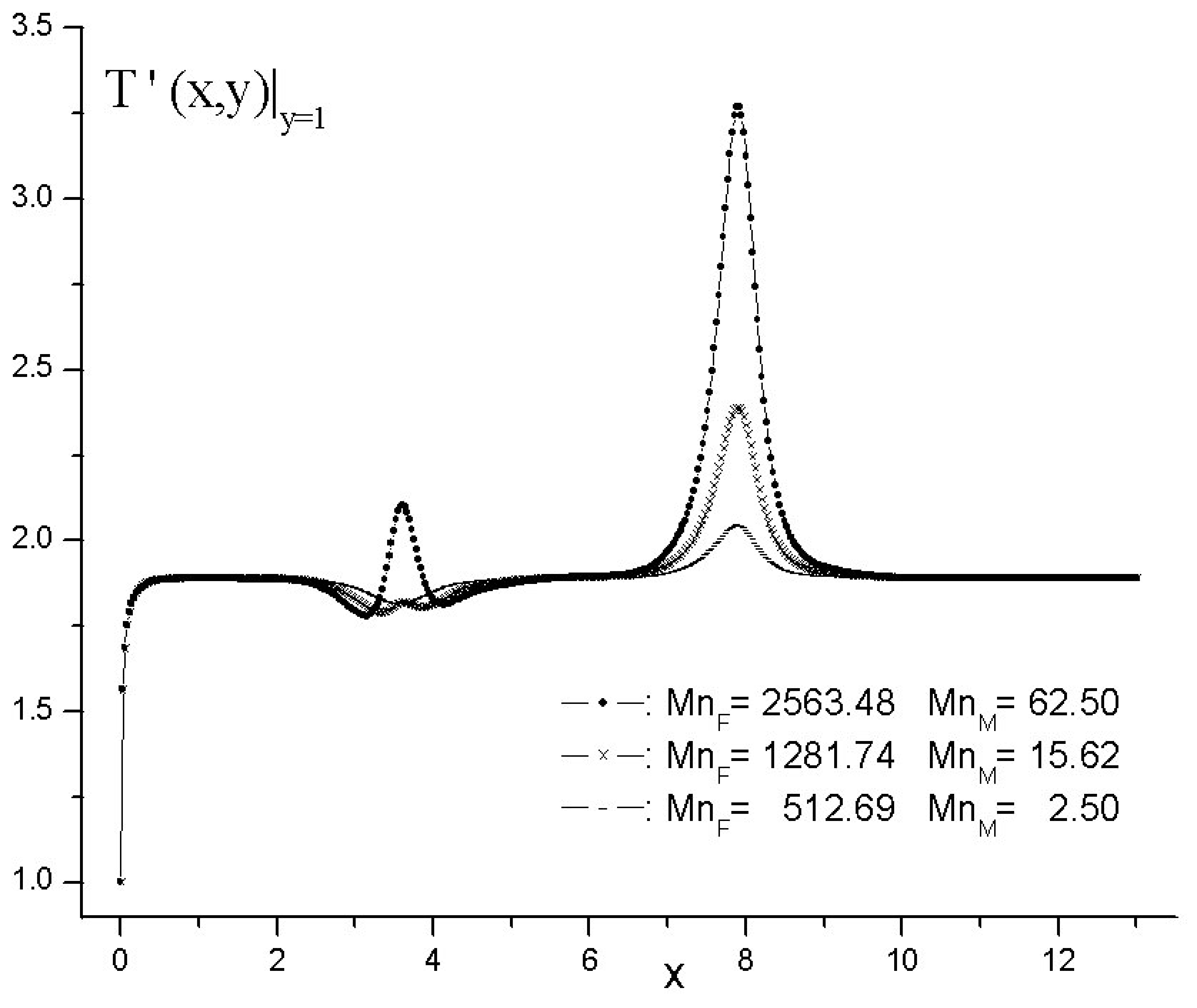

3.5
3.0
2.5
2.0
1.5
1.0
T ' (x,y)|y=1
: MnF= 2563.48 MnM= 62.50
: MnF= 1281.74 MnM= 15.62
: MnF= 512.69 MnM= 2.50
0
2
4
6
8
10
12
x

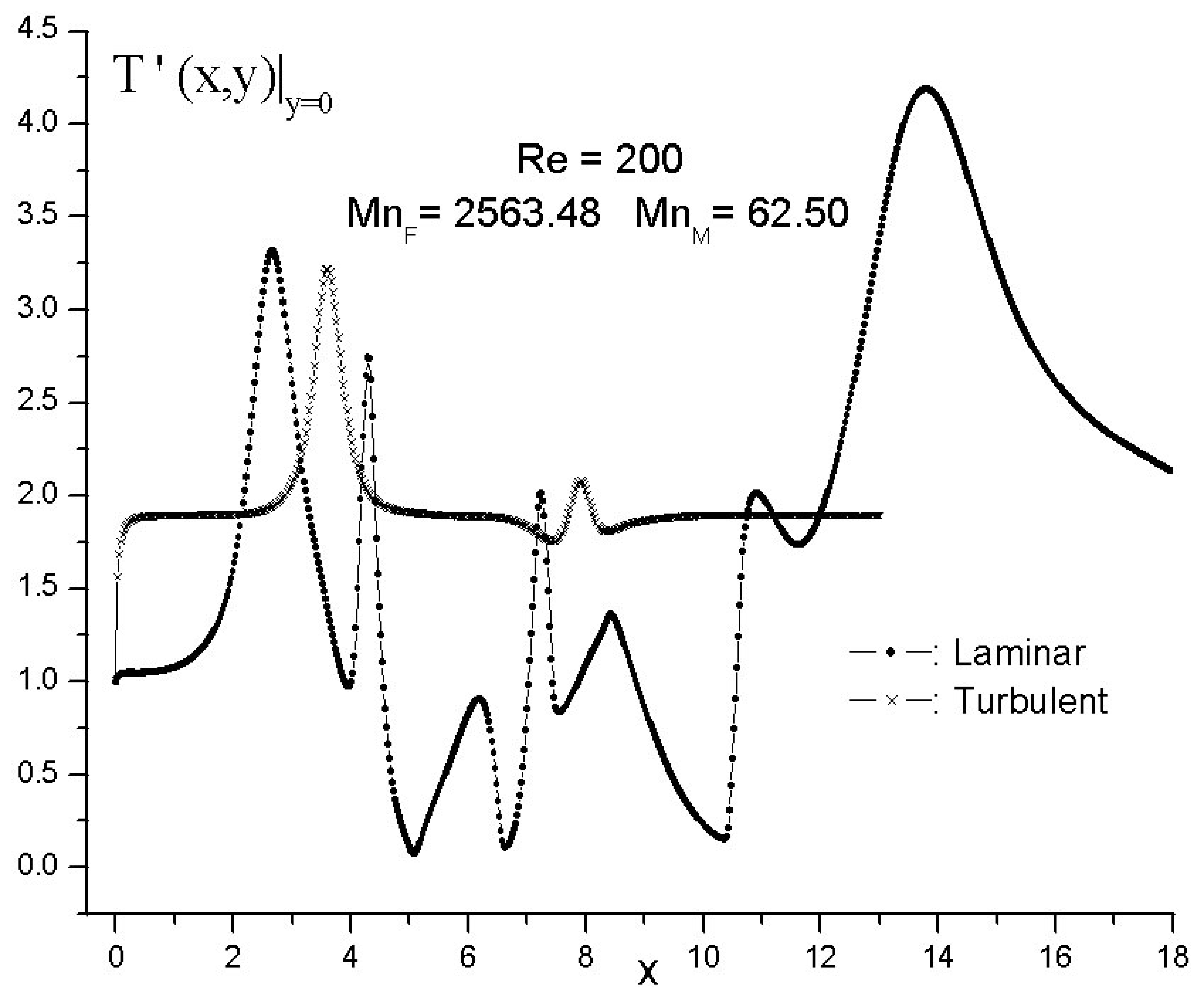

T ' (x,y)|y=0
Re = 200
MnF = 2563.48 MnM = 62.50
: Laminar
: Turbulent
x
0
2
4
6
8
10
12
14
16
18
0.0
0.5
1.0
1.5
2.0
2.5
3.0
3.5
4.0
4.5

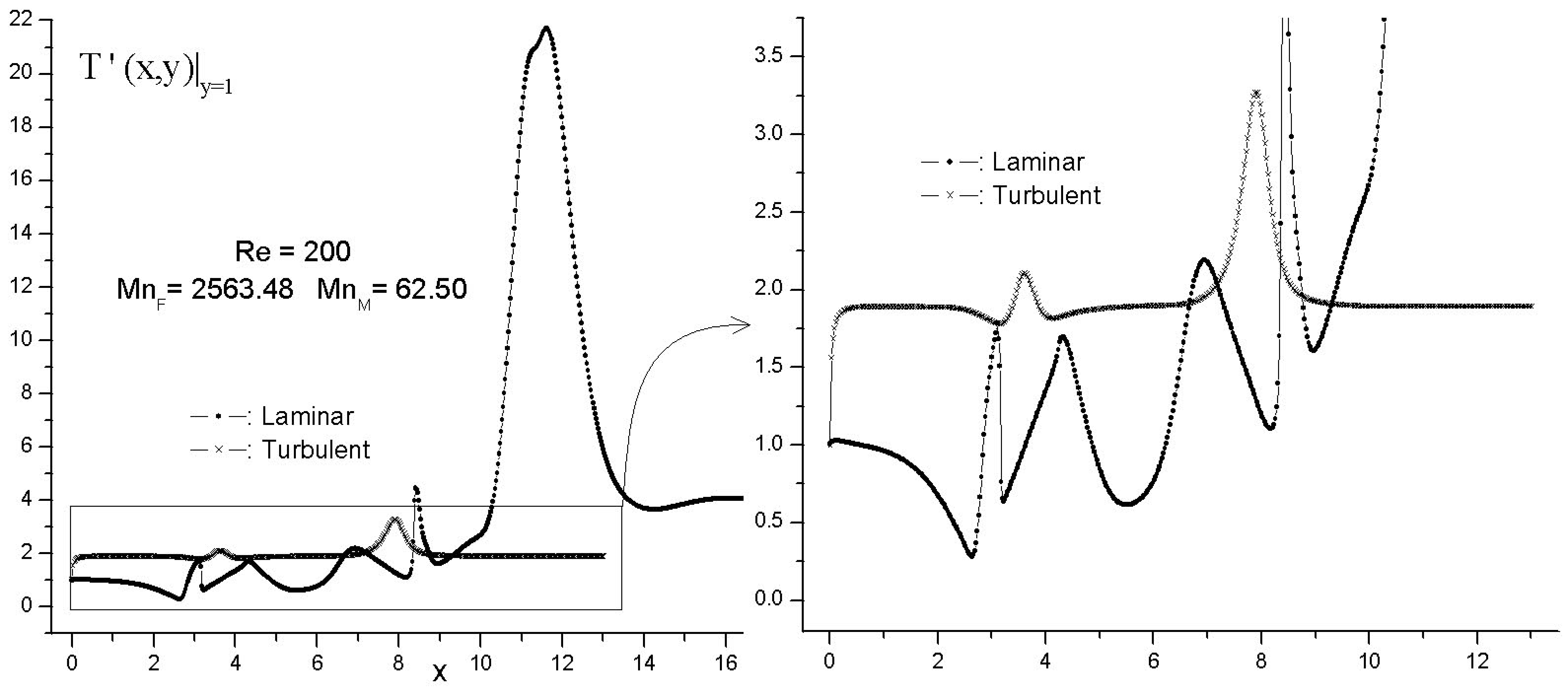
$T'(x,y)|_{y=1}$
Re = 200
Mn_F = 2563.48 Mn_M = 62.50
—•—: Laminar
—×—: Turbulent
x
—•—: Laminar
—×—: Turbulent